J|A|C|S
ARTICLES
Published on Web 04/29/2006

Reversible Photoswitching of the Coordination Numbers of Silicon in Organosilicon Compounds Bearing a 2-(Phenylazo)phenyl Group

Naokazu Kano, Fuminori Komatsu, Masaki Yamamura, and Takayuki Kawashima*

Contribution from the Department of Chemistry, Graduate School of Science, The University of Tokyo, 7-3-1 Hongo, Bunkyo-ku, Tokyo 113-0033, Japan

Received February 8, 2006; E-mail: takayuki@chem.s.u-tokyo.ac.jp

Abstract: Several organosilicon compounds bearing a 2-(phenylazo)phenyl group were synthesized from the corresponding chlorosilanes and 2-lithioazobenzene prepared by halogen−lithium transmetalation of 2-iodoazobenzene. Their structures were determined by ^{1}H, ^{13}C, ^{19}F, and ^{29}Si NMR spectra, UV−vis spectra, and X-ray crystallographic analyses. In the UV−vis spectra, silyl groups caused red shifts of both the n−π^* and π−π^* transitions of the azo group compared with the transitions of the unsubstituted azobenzene. The *E*-isomers of the fluorosilanes showed an intramolecular interaction between a nitrogen atom of the azo group and the silicon atom, leading their intermediate structures between a distorted trigonal bipyramidal structure and a tetrahedral structure around the silicon atoms, which were revealed by the X-ray crystallographic analyses and the NMR spectra. On the other hand, silanes without fluorine atoms showed tetrahedral structures in the absence of such an interaction. The photoirradiation of the *E*-isomers of the fluorosilanes afforded reversibly the corresponding *Z*-isomers in good yields. The silicon atoms of the *Z*-isomers were found to be tetracoordinate in the absence of Si−N interactions by the ^{29}Si NMR spectra. The coordination numbers of the silicon atom of the fluorosilanes were reversibly switched between four and five by photoirradiation. These properties were compared to those of a tetrafluoro[2-(phenylazo)phenyl]-silicate.

Introduction

Pentacoordinate organosilicon compounds have been studied very much because of their interesting structures, properties, and reactivities, some of which are different from those of tetracoordinate ones.[1] For example, some substituents on a pentacoordinate silicon atom are more nucleophilically activated than those on a tetracoordinate one.[1c,2] Reversible change from a tetracoordinated and tetrahedral structure to a pentacoordinated and trigonal bipyramidal (TBP) structure by addition and elimination of a fluoride anion has been reported to be useful for the construction and decomposition of a conjugation system.[3] If the tetracoordination state of a silicon atom in a neutral tetravalent organosilicon compound could be reversibly changed to a pentacoordination state in response to an external stimulus without addition of any external reagents at the same temperature, its structure and various properties would be controlled in company with the coordination number of its silicon atom (Scheme 1).

Scheme 1

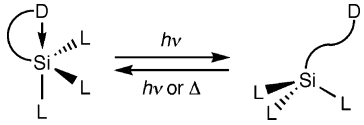

Stable neutral pentacoordinate organosilanes usually have a heteroatom tether such as nitrogen and oxygen in the vicinity of the silicon atom, so that the silicon atom shows a pentacoordination state with an intramolecular interaction between the heteroatom and the silicon atom. The coordination states can easily be changed depending on the conditions such as temperature.[4] Thus, it is difficult to control the coordination numbers of neutral organosilicon compounds between four and five under certain conditions in the case where the coordination site is fixed rigidly near the silicon atom or loosely contacted to the silicon atom.[5] There are some reports on the control of equilibrium between the pentacoordinate and hexacoordinate organosilicon

(1) (a) Chuit, C.; Corriu, R. J. P.; Reye, C.; Young, J. C. In *The Chemistry of Organic Silicon Compounds, Part 1*; Patai, S., Rappoport, Z., Eds.; Wiley: Chichester, 1989; pp 1241−1288. (b) Holmes, R. R. *Chem. Rev.* **1990**, *90*, 17. (c) Chuit, C.; Corriu, R. J. P.; Reye, C.; Young, J. C. *Chem. Rev.* **1993**, *93*, 1371. (d) Wong, C. Y.; Woolins, J. D. *Coord. Chem. Rev.* **1994**, *130*, 175. (e) Holmes, R. R. *Chem. Rev.* **1996**, *96*, 927. (f) Chuit, C.; Corriu, R. J. P.; Reye, C. In *Chemistry of Hypervalent Compounds*; Akiba, K.-y., Ed.; Wiley-VCH: New York, 1999; pp 81−146. (g) Kira, M.; Zhang, L.-C. In *Chemistry of Hypervalent Compounds*; Akiba, K.-y., Ed.; Wiley-VCH: New York, 1999; pp 147−169. (h) Kost, D.; Kalikhman, I. In *The Chemistry of Organic Silicon Compounds, Volume 2, Part 2*; Patai, S., Apeloig, Y., Eds.; John Wiley & Sons: Chichester, 1998; pp 1339−1445.

(2) Corriu, R. J. P.; Lanneau, G. F.; Perrot, M. *Tetrahedron Lett.* **1988**, *29*, 1271.

(3) Yamaguchi, S.; Akiyama, S.; Tamao, K. *J. Am. Chem. Soc.* **2000**, *122*, 6793.

(4) (a) Helmer, B. J.; West, R.; Corriu, R. J. P.; Poirier, M.; Royo, G.; de Saxce, A. *J. Organomet. Chem.* **1983**, *251*, 295. (b) Brelière, C.; Carré, F.; Corriu, R. J. P.; Douglas, W. E.; Poirier, M.; Royo, G.; Wong Chi Man, M. *Organometallics* **1992**, *11*, 1586.

(5) Brelière, C.; Carré, F.; Corriu, R. J. P.; Poirier, M.; Royo, G. *Organometallics* **1986**, *5*, 388.

species by changing temperature, solvents, and counterions.[6] However, the process of the coordination-number change should be carried out under constant reaction conditions in order to achieve reactivity control by the coordination-number change alone without any additive and without changing the temperature and the solvent.

An azobenzene, which is expected to work as a chromophore and a structural changing unit, is well utilized for the photoswitching of various functions and properties.[7] An azobenzene framework has been used as a bidentate ligand in some transition metal complexes.[8] In the (*E*)-form of a 2-silyl substituted azobenzene, the nitrogen atom is expected to coordinate to the silicon atom and form a five-membered ring, which should suitably stabilize the pentacoordination state of the silicon. We previously reported photoswitching of the coordination numbers of the silicon between five and six in anionic silicon compounds bearing a 2-(phenylazo)phenyl group.[9] The intramolecular coordination of an azo unit would be also applicable to photoswitching of the coordination numbers of the silicon between usual and high coordination states, that is, between tetracoordinate and pentacoordinate structures. Although there have been some methods for the syntheses of azobenzenes bearing a silicon substituent under basic or acidic conditions, these reaction conditions are unsuitable for the syntheses of the fluorosilanes, in which a pentacoordination state is expected to be stabilized.[10,11] The 2-(phenylazo)phenyl group is expected to work both as a chromophore and a coordination site toward the silicon atom. Actually, we have applied this method to the syntheses of a disiloxane and an allylsilane bearing an azobenzene moiety.[12,13]

We report here full details of the synthetic methods, structures, and spectral properties of several neutral organosilanes bearing one or two azobenzene moieties and the tetrafluorosilicate. We also report reversible photocontrol of the coordination numbers of the silicon atom between four and five in neutral fluorosilanes.

Synthesis

Lithium−halogen transmetalation of 2-haloazobenzene was carried out in a manner similar to lithiation of 4-bromo-4′-ethylazobenzene.[14] Treatment of 2-bromoazobenzene ((*E*)-**1a**) with *n*-BuLi (1.05 equiv) and chlorotrimethylsilane (1.05 equiv) successively in THF at −105 °C gave the corresponding 2-trimethylsilylazobenzene ((*E*)-**2a**) in 25% yield. The low yield of (*E*)-**2a** is ascribed to the formation of both 1-(2-bromophenyl)-1-butyl-2-phenylhydrazine and 1-(2-bromophenyl)-2-butyl-2-phenylhydrazine, which were confirmed by GC−MS (*m*/*z* 318) as byproducts. Lithiation of 2-iodoazobenzene ((*E*)-**1b**) instead of (*E*)-**1a** generated 2-lithioazobenzene more efficiently, and successive treatment of chlorotrimethylsilane afforded (*E*)-**2a** in a satisfactory yield (80%). Keeping the reaction temperature at −105 °C during the addition of *n*-BuLi is important to avoid its attack on the azo group; otherwise the yield of (*E*)-**2a** becomes low. Several 2-silylazobenzene derivatives were synthesized by this method (Scheme 2). Dimethylphenylsilyl derivative (*E*)-**2b** was synthesized in a good yield (92%), while methyldiphenylsilyl derivative (*E*)-**2c** was obtained in a low yield (29%). Triphenylsilyl derivative was not obtained in the reaction with chlorotriphenylsilane probably due to the steric hindrance. Triethoxysilane (*E*)-**2d**, monohydrosilanes (*E*)-**2e** and (*E*)-**2f**, and diethoxysilane (*E*)-**2g** were also synthesized in moderate yields, 75, 63, 79, and 49% yields, respectively. Use of 0.52 equiv of dichlorodimethylsilane, dichlorodiphenylsilane, and dichlorophenylsilane as electrophiles in the reactions of the aryllithium gave the corresponding bis[2-(phenylazo)phenyl]silanes, (*E*,*E*)-**3a** (89%), (*E*,*E*)-**3b** (70%), and (*E*,*E*)-**3c** (56%), respectively. Fluorination of triethoxysilane (*E*)-**2d** and diethoxysilane (*E*)-**2g** with BF_3·OEt_2 proceeded smoothly to give trifluorosilane (*E*)-**4d** (49%) and difluorosilane (*E*)-**4g** (67%), respectively (Scheme 3). Further fluorination of (*E*)-**4d** with KF (1.0 equiv) in the presence of 18-crown-6 gave tetrafluorosilicate (*E*)-**5**

Scheme 2

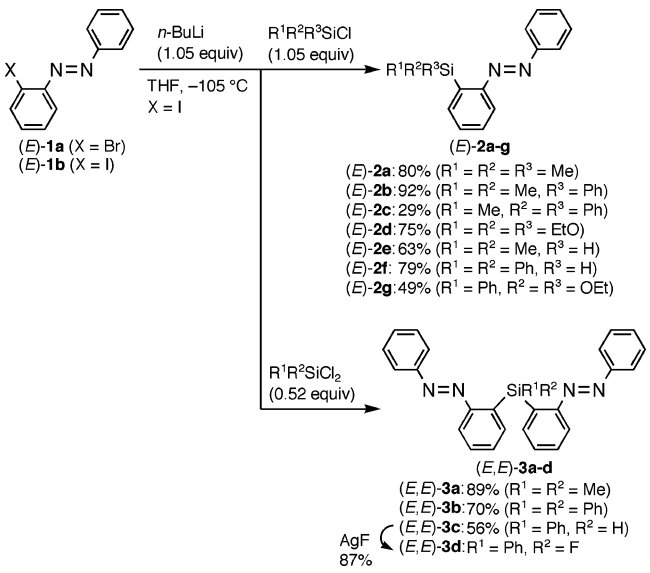

Scheme 3

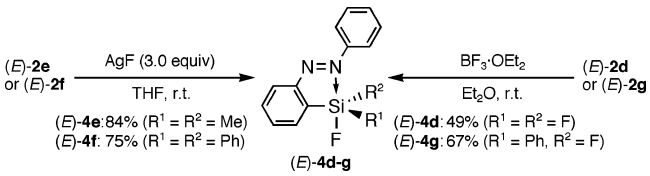

(6) (a) Kalikhman, I.; Girshberg, O.; Lameyer, L.; Stalke, D.; Kost, D. *J. Am. Chem. Soc.* **2001**, *123*, 4709. (b) Kingston, V.; Gostevskii, B.; Kalikhman, I.; Kost, D. *Chem. Commun.* **2001**, 1272. (c) Kost, D.; Kalikhman, I.; Kingston, V.; Gostevskii, B. *J. Phys. Org. Chem.* **2002**, *15*, 831. (d) Kost, D.; Kingston, V.; Gostevskii, B.; Ellern, A.; Stalke, D.; Walfort, B.; Kalikhman, I. *Organometallics* **2002**, *21*, 2293. (e) Kalikhman, I.; Gostevskii, B.; Girshberg, O.; Krivonos, S.; Kost, D. *Organometallics* **2002**, *21*, 2551. (f) Kalikhman, I.; Gostevskii, B.; Girshberg, O.; Sivaramakrishna, A.; Kocher, N.; Stalke, D.; Kost, D. *J. Organomet. Chem.* **2003**, *686*, 202. (g) Gostevskii, B.; Adear, K.; Sivaramakrishna, A.; Silbert, G.; Stalke, D.; Kocher, N.; Kalikhman, I.; Kost D. *Chem. Commun.* **2004**, 1644. (h) Wagler, J.; Böhme, U.; Brendler, E.; Roewer, G. *Z. Naturforsch.* **2004**, *59b*, 1348. (i) Kost, D.; Kalikhman, I. *Adv. Organomet. Chem.* **2004**, *50*, 1. (j) Nakash, M.; Goldvaser, M. *J. Am. Chem. Soc.* **2004**, *126*, 3436. (k) Wagler, J.; Böhme, U.; Brendler, E.; Roewer, G. *Organometallics* **2005**, *24*, 1348. (k) Gostevskii, B.; Silbert, G.; Adear, K.; Sivaramakrishna, A.; Stalke, D.; Deuerlein, S.; Kocher, N.; Voronkov, M. G.; Kalikhman, I.; Kost, D. *Organometallics* **2005**, *24*, 2913.

(7) (a) *Molecular Switches*; Feringa, B. L., Ed.; Wiley-VCH: Weinheim, 2001. (b) *Molecular Devices and Machines*; Balzani, V., Venturi, M., Credi, A., Eds.; Wiley-VCH: Weinheim, 2003.

(8) (a) Fahey, D. R. *J. Chem. Soc., Chem. Commun.* **1970**, 417. (b) Fahey, D. R. *J. Organomet. Chem.* **1971**, *27*, 283. (c) Bruce, M. I.; Goodall, B. L. In *The Chemistry of the Hydrazo, Azo and Azoxy Groups, Part 1*; Patai, S., Ed.; John Wiley & Sons: New York, 1975; pp 259−311. (d) Omae, I. *Chem. Rev.* **1979**, *79*, 287.

(9) Kano, N.; Komatsu, F.; Kawashima, T. *J. Am. Chem. Soc.* **2001**, *123*, 10778.

(10) Sunthankar, S. V.; Gilman, H. *J. Org. Chem.* **1950**, *15*, 1200.

(11) Kano, N.; Komatsu, F.; Kawashima, T. *Chem. Lett.* **2001**, 338.

(12) Kano, N.; Yamamura, M.; Komatsu, F.; Kawashima, T. *J. Organomet. Chem.* **2003**, *686*, 192.

(13) Kano, N.; Yamamura, M.; Kawashima, T. *J. Am. Chem. Soc.* **2004**, *126*, 6250.

(14) Kozlecki, T.; Syper, L.; Wilk, K. A. *Synthesis* **1997**, 681.

Scheme 4

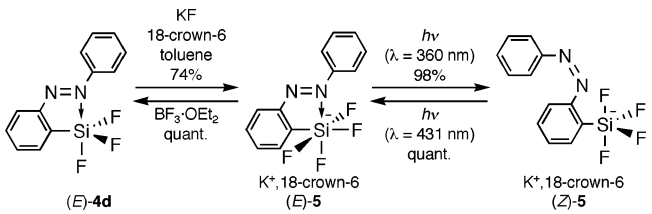

(74%) (Scheme 4). Hydrosilanes (*E*)-**2e**, (*E*)-**2f**, and (*E*,*E*)-**3c** were further converted to the corresponding fluorosilanes (*E*)-**4e** (84%), (*E*)-**4f** (75%), and (*E*,*E*)-**3d** (87%), respectively, by treatment with silver fluoride in THF (Schemes 2 and 3).

NMR Spectral Properties

The ^{1}H, ^{13}C, ^{19}F, and ^{29}Si NMR spectra of (*E*)-**2a**−**g**, (*E*,*E*)-**3a**−**d**, (*E*)-**4d**−**g**, and (*E*)-**5** were measured to clarify their structures and coordination states of their silicon atoms. The ^{29}Si NMR chemical shifts (δ_{Si}) are summarized in Table 1 and compared with those of the corresponding phenyl-substituted references (δ_{Si}').[5,15,16] In the ^{29}Si NMR spectra, each chemical shift of (*E*)-**2a**−**g** and (*E*,*E*)-**3a,b** is near those of the corresponding phenyl-substituted derivatives. The respective differences of the chemical shifts ($\Delta\delta_{Si} = \delta_{Si} - \delta_{Si}'$) between (*E*)-**2a**−**g** and the corresponding phenyl derivatives are less than 3 ppm. Considering the small $\Delta\delta_{Si}$ values, (*E*)-**2a**−**g** and (*E*,*E*)-**3a,b** possess tetracoordinate silicon atoms in the absence of Si···N interaction. Steric repulsion between the silyl groups and a PhN moiety should prevent the Si···N interaction.

Compound (*E*,*E*)-**3c** showed spectral behavior slightly different from these silanes. In the ^{29}Si NMR spectra, the signal due to (*E*,*E*)-**3c** (δ_{Si} −23.2) was observed in a higher field than that of triphenylsilane (δ_{Si} −17.8) by about 5 ppm. Considering that the electronic perturbation through the C−Si bond in the hydrosilane is as little as those in (*E*)-**2a**−**g** and (*E*,*E*)-**3a,b**, the differences of the chemical shifts should be attributed to the contribution of a pentacoordination state of the silicon atom with a Si···N interaction in (*E*,*E*)-**3c** in the solution state.

Differences in the ^{29}Si NMR chemical shifts between 2-(phenylazo)phenyl derivatives and the corresponding phenyl derivatives are notable in fluorosilanes. In the ^{29}Si NMR spectra, trifluorosilane (*E*)-**4d** and difluorosilane (*E*)-**4g** showed a quartet and a triplet by coupling with fluorine nuclei at δ_{Si} −91.2 ($^{1}J_{SiF}$ = 231.0 Hz) and −47.8 ($^{1}J_{SiF}$ = 264.5 Hz), respectively. Each of the monofluorosilanes (*E*)-**4e**, (*E*)-**4f**, and (*E*,*E*)-**3d** showed a doublet by coupling with a fluorine nucleus at δ_F 8.3 ($^{1}J_{SiF}$ = 267.7 Hz), δ_F −16.3 ($^{1}J_{SiF}$ = 273.6 Hz), and δ_F −17.3 ($^{1}J_{SiF}$ = 273.2 Hz), respectively. Fluorosilanes (*E*)-**4d**, (*E*)-**4g**, (*E*,*E*)-**3d**, (*E*)-**4e**, and (*E*)-**4f** showed upfield shifts of about 12 ppm compared to the corresponding trifluorophenylsilane (δ_{Si} −73.7), difluorodiphenylsilane (δ_{Si} −30.5), fluorodimethylphenylsilane (δ_{Si} −19.8), and fluorotriphenylsilane (δ_{Si} −4.7), respectively, so that they are considered to have pentacoordination states in the solution states.[16] The $\Delta\delta_{Si}$ values increase in the order of numbers of fluorine atoms on the silicon atom. The electron-withdrawing fluorine atoms raise the Lewis acidity of the silicon atom, and the Si···N interactions become stronger in accordance with the number of the fluorine atoms.

Table 1. ^{29}Si NMR Data (δ_{Si}) and the λ_{max} in the UV−vis Spectra of Organosilicon Compounds Bearing One or Two 2-(Phenylazo)phenyl Group(s), the ^{29}Si NMR Data (δ_{Si}') of the Corresponding Phenyl-Substituted Compounds, and the Differences ($\Delta\delta_{Si}$) of the ^{29}Si Chemical Shifts

		λ_{max}/nm (ϵ)[b]				
nos.	δ_{Si}[a]	π–π^*	n–π^*	references	δ_{Si}'	$\Delta\delta_{Si}$
(*E*)-**2a**	−4.0	325 (16 000)	450 (460)	Me_3PhSi	−4.1[c]	+0.1
(*E*)-**2b**	−7.5	325 (24 000)	453 (770)	Me_2Ph_2Si	−8.6[d]	+1.1
(*E*)-**2c**	−10.3	326 (24 000)	455 (500)	$MePh_3Si$	−12.1[d]	+1.8
(*E*)-**2d**	−58.1	325 (17 000)	450 (600)	$(EtO)_3PhSi$	−57.8[c]	−0.3
(*E*)-**2e**	−17.0	325 (15 000)	448 (410)	Me_2PhHSi	−17.6[e]	+0.6
(*E*)-**2f**	−19.9	327 (21 000)	451 (570)	Ph_3HSi	−17.8[e]	−2.1
(*E*)-**2g**	−32.6	325 (19 000)	450 (520)	$Ph_2(EtO)_2Si$	−32.4[d]	−0.2
(*E*,*E*)-**3a**	−7.8	326 (39 000)	456 (960)	Me_2Ph_2Si	−8.6[d]	+0.8
(*E*,*E*)-**3b**	−13.8	326 (38 000)	457 (1000)	Ph_4Si	−14.0[d]	+0.2
(*E*,*E*)-**3c**	−23.2	327 (33 000)	454 (770)	Ph_3HSi	−17.8[e]	−5.4
(*E*,*E*)-**3d**	−17.3	326 (37 000)	441 (1000)	Ph_3FSi	−4.7[e]	−12.6
(*E*)-**4d**	−91.2	345 (24 000)		PhF_3Si	−73.7[e]	−17.5
(*E*)-**4e**	8.3	328 (19 000)	434 (640)	Me_2PhFSi	19.8[e]	−11.5
(*E*)-**4f**	−16.3	336 (20 000)	436 (700)	Ph_3FSi	−4.7[e]	−11.6
(*E*)-**4g**	−47.8	349 (20 000)		Ph_2F_2Si	−30.5[e]	−17.3
(*Z*)-**4d**	−70.6		336 (2000)[f]	PhF_3Si	−73.7[e]	3.1
(*Z*)-**4e**	21.0	294 (7100)	444 (1900)	Me_2PhFSi	19.8[e]	1.3
(*Z*)-**4f**	−7.3	288 (8000)	445 (2000)	Ph_3FSi	−4.7[e]	−2.6
(*Z*)-**4g**	−29.8	286 (8000)	445 (2000)	Ph_2F_2Si	−30.5[e]	0.7
(*E*)-**5**	−150.9	334 (19 000)		PhF_4Si^-, K^+	−125.8[g]	−25.1
(*Z*)-**5**	−122.8	277 (6500)	433 (1800)	PhF_4Si^-, K^+	−125.8[g]	3.0

[a] In $CDCl_3$. [b] In CH_2Cl_2. [c] Reference 5. [d] Reference 15. [e] Reference 16. [f] In THF. [g] Reference 17.

The upfield shifts in the ^{29}Si NMR were also observed in tetrafluorosilicate (*E*)-**5**. In the ^{29}Si NMR spectra, (*E*)-**5** showed a quintet ($^{1}J_{SiF}$ = 193 Hz) at δ −150.9 by coupling with four equivalent fluorine nuclei at rt in $CDCl_3$. The signal split to a doublet of double triplet at δ −153.7 coupled with three kinds of nuclei ($^{1}J_{SiF}$ = 149, 186, and 214 Hz, respectively) at −90 °C in CD_2Cl_2. The chemical shift is observed in a much higher field than that of potassium tetrafluorophenylsilicate (δ −125.8)[17] and one similar to those of a hexacoordinate tetrafluorosilicate bearing a 2-(*N*,*N*-dimethylaminomethyl)phenyl group,[4b] indicating the hexacoordination state of the silicon atom due to the coordination of the nitrogen atom of the azo group.

The pentacoordination states of some of these fluorosilanes were confirmed by VT-^{19}F NMR spectra. In the ^{19}F NMR spectra of (*E*)-**4g** in $CDCl_3$, a singlet at δ_F −141.55 with satellite peaks ($^{1}J_{SiF}$ = 268.4 Hz) at rt was split into two broad peaks at δ_F −148.66 (1F) and −133.43 (1F) at −70 °C. Similarly, in the ^{19}F NMR spectra of (*E*)-**4d**, a broad singlet at δ_F −140.58 with satellite peaks ($^{1}J_{SiF}$ = 234.9 Hz) in CD_2Cl_2 at rt was split to a doublet at δ_F −140.11 ($^{2}J_{FF}$ = 52.0 Hz) and a triplet at δ_F −136.79 ($^{2}J_{FF}$ = 52.0 Hz) in the ratio of 2:1 at −90 °C. Similarly, a broad singlet of (*E*)-**5** at δ −127.4 in $CDCl_3$ at rt was split to two broad signals (δ −122.5 and −147.2) at −30 °C in CD_2Cl_2. They were further split to a pair of doublets at δ −121.6 ($^{2}J_{FF}$ = 21.3 Hz) and −123.2 ($^{2}J_{FF}$ = 24.4 Hz) and one double-triplet at δ −147.2 ($^{2}J_{FF}$ = 21.3 Hz, $^{2}J_{FF}$ = 24.4 Hz) at −90 °C, respectively, in CD_2Cl_2.

Such behaviors of the chemical shifts and the coupling patterns indicate the nonequivalency of fluorine atoms due to the coordination of a nitrogen atom of the azo group furnishing TBP geometry around the pentacoordinate silicon atom in (*E*)-**4d** and (*E*)-**4g** and octahedral geometry around the hexacoordinate silicon atom in (*E*)-**5**.[5,18] Fast pseudorotation of the

(15) Cragg, R. H.; Lane, R. D. *J. Organomet. Chem.* **1984**, *277*, 199.
(16) Williams, E. A.; Cargioli, J. D. In *Annual Reports on NMR Spectroscopy*; Webb, G. A., Ed.; Academic Press: New York, 1979; Vol. 9.
(17) Swamy, K. C. K.; Chandrasekhar, V.; Harland, J. J.; Holmes, J. M.; Day, R. O.; Holmes, R. R. *J. Am. Chem. Soc.* **1990**, *112*, 2341.

ligands compared to the time scale of NMR spectroscopy would result in observation of a singlet in the ^{19}F NMR spectra at rt.

X-ray Crystallographic Analyses of (*E*)-Isomers

The crystal structures of (*E*)-**2c**, (*E*)-**2f**, (*E*,*E*)-**3a**, (*E*)-**4d**, (*E*)-**4f**, (*E*)-**4g**, and (*E*)-**5** were determined by X-ray crystallographic analyses. Their crystallographic data and selected bond lengths (Å) and angles (deg) are summarized in Tables 2 and 3, respectively. Their ORTEP drawings are shown in Figures 1−7.

In (*E*)-**2c**, (*E*)-**2f**, and (*E*,*E*)-**3a**, the silyl group and N2 atom are arranged in a trans fashion with regard to the C6−N1 bond (Figures 1−3). Steric repulsion between the bulky silyl group and a PhN moiety overcomes attractive electrostatic intramolecular Si···N interaction. The intramolecular interaction cannot defeat the steric repulsion even in hydrosilane (*E*)-**2f** bearing a sterically less bulky silyl group.[11] Even though (*E*,*E*)-**3a** has two 2-(phenylazo)phenyl groups, one of which might coordinate to Si1 atom, the other two methyl groups do not help the coordination and there is no Si···N interaction in it. Apparently, (*E*)-**2c**, (*E*)-**2f**, and (*E*,*E*)-**3a** should be regarded as tetrahedral structures around their silicon atoms.

In (*E*)-**4d**, (*E*)-**4f**, and (*E*)-**4g**, the N2 atoms are directed to the Si1 atoms despite the steric repulsion (Figures 4−6). The intramolecular N2···Si1 distance of (*E*)-**4d** (2.3030(14) Å) is almost the same as those of [8-(*N*,*N*-dimethylamino)naphthyl]-trifluorosilane (2.287(4) and 2.318(6) Å for two independent molecules).[19] The intramolecular N2···Si1 distance of difluorosilane (*E*)-**4g** (2.419(2) Å) is slightly longer than that of [2-(*N*,*N*-dimethylaminomethyl)phenyl]difluoromethylsilane (2.346(3) Å).[20] The intramolecular N2···Si1 distance of monofluorosilane (*E*)-**4f** (2.605(2) Å) is apparently shorter than that of 1-fluoro-1,2-dimethyl-1-[8-(*N*,*N*-dimethylamino)naphthyl]-2,2-diphenyldisilane (2.852(2) Å).[21] They are much shorter than the sum of the van der Waals radii of Si and N (3.65 Å). Taking into consideration that a hypervalent bond is generally longer than the sum of the covalent radii and that the lone pair of the N2 atom heads for the σ^* orbital of the Si1−F1 bond, intramolecular N2···Si1 interactions evidently exist in (*E*)-**4d**, (*E*)-**4f**, and (*E*)-**4g**. Their N2···Si1 interactions furnish them with pentacoordination states of the silicon atoms in the crystalline states. A similar Si−N dative bond was observed in tetrafluorosilicate (*E*)-**5** (Figure 7).[9] The intramolecular N2···Si1 distance in (*E*)-**5** is 2.2498(13) Å. The differences in their interatomic Si···N distances in order of (*E*)-**5** > (*E*)-**4d** > (*E*)-**4g** > (*E*)-**4f** can be rationalized by the electron deficiency of the silicon atoms and the steric accessibility to the silicon atoms in this order, whereas the silicon atom of (*E*)-**5** is more sterically congested than that of (*E*)-**4d**. Accordingly, N2···Si1−F1 bond angles [(*E*)-**4d**, 176.62(6)°; (*E*)-**5**, 175.65(5)°; (*E*)-**4g**, 172.78(5)°; (*E*)-**4f**, 170.27(5)°] are in the order of the interatomic Si···N distances except (*E*)-**5**. The structures of (*E*)-**4d**, (*E*)-**4f**, and (*E*)-**4g** are interpreted as the intermediate between the tetrahedral structure and TBP structure with N2 and F1 atoms at apical positions. One reason for the deviation from an ideal TBP structure is rigidity of the 2-(phenylazo)phenyl group which contains benzo and azo units in a five-membered ring framework and hence forces the nitrogen atom to coordinate from the slanted backside of the Si−F bond. Similarly, the structure of (*E*)-**5** is interpreted as a distorted octahedral configuration suggested by the bond angles (76.41(6)°−99.47(6)°) around the Si1 atom. A calculation of the extent that the Si1···N2 distance [2.2498(13) Å] is displaced from the sum of the van der Waals radii of 3.65 Å to the sum of the covalent radii of 1.87 Å for silicon and nitrogen provides an estimate of the octahedral character of (*E*)-**5** of 79%.[22]

We tried to estimate the structural deviation of these fluorosilanes from an ideal TBP structure. The pentacoordination characters, $\%TBP_a$ and $\%TBP_e$, have been used as indicators of the structure about the central element in terms of the percentage TBP geometry along a tetrahedron→TBP reaction coordinate based on the apical-element-equatorial bond angles and equatorial-element-equatorial bond angles, respectively.[23,24] The pentacoordination characters, $\%TBP_a$ and $\%TBP_e$, are defined by the following eqs 1 and 2, where θ_n and φ_n are the angles $L_{ap}-Si-L_{eq}$ and $L_{eq}-Si-L_{eq}$, respectively. For the pentacoordination characters of the Si1 atom, L_{ap} is the F1 atom in (*E*)-**4d**, (*E*)-**4f**, and (*E*)-**4g**. For the pentacoordination characters of the Si1 atom, L_{eq} are C1, F2, and F3 atoms in (*E*)-**4d**, L_{eq} are C1, C13, and C19 atoms in (*E*)-**4f**, and L_{eq} are C1, C13, and F2 atoms in (*E*)-**4g**, respectively.

$$\%TBP_a = \left\{109.5° - \frac{1}{3}\left(\sum_{n=1}^{3}\theta_n\right)\right\}/(109.5° - 90°) \times 100 \quad (1)$$

$$\%TBP_e = \left\{\frac{1}{3}\left(\sum_{n=1}^{3}\varphi_n\right) - 109.5°\right\}/(120° - 109.5°) \times 100 \quad (2)$$

The pentacoordination characters, $\%TBP_a$ and $\%TBP_e$, were calculated to be 53% and 76% for (*E*)-**4d**, 53% and 76% for (*E*)-**4f**, and 48% and 71% for (*E*)-**4g**, respectively. These values suggest that the configuration around the silicon atoms are intermediate structures between tetrahedral and TBP structures. They are comparable with the pentacoordination characters of previously reported pentacoordinate fluorosilanes such as [2-(*N*,*N*-dimethylaminomethyl)phenyl]difluoromethylsilane ($\%TBP_a$, 61% and $\%TBP_e$, 83%)[20] and 1-fluoro-1,2-dimethyl-1-[8-(*N*,*N*-dimethylamino)naphthyl]-2,2-diphenyldisilane ($\%TBP_a$, 57% and $\%TBP_e$, 80%).[21,25] Although the Si···N distances are in the order of the number of fluorine atoms on the silicon atom for (*E*)-**4d**, (*E*)-**4f**, and (*E*)-**4g**, the %TBP characters are not in this order. Since the %TBP values are most effective in the case of the intramolecular coordinating ligands which coordinate from right behind the Si−F bond, they are not good for estimating the TBP characters of (*E*)-**4d**, (*E*)-**4f**, and (*E*)-**4g**, in which N2 atoms coordinate to Si1 atoms obliquely from behind.

The N1−N2 bond lengths of (*E*)-**2c**, (*E*)-**2f**, and (*E*,*E*)-**3a** [1.2515(16)−1.2580(18) Å] are almost the same as the average dimensions (1.25 Å) of previously reported (*E*)-azobenzenes,[26,27]

(18) (a) Breliere, C.; Carre, F.; Corriu, R. J. P.; de Saxce, A.; Poirier, M.; Royo, G. *J. Organomet. Chem.* **1981**, *205*, C1. (b) Boyer, J.; Brelière, C.; Carré, F.; Corriu, R. J. P.; Kpoton, A.; Poirier, M.; Royo, G.; Young, J. C. *J. Chem. Soc., Dalton Trans.* **1989**, 43. (c) Corriu, R. J. P.; Kpoton, A.; Poirier, M.; Royo, G.; de Saxcé, A.; Young, J. C. *J. Organomet. Chem.* **1990**, *395*, 1.
(19) Carré, F.; Corriu, R. J. P.; Kpoton, A.; Poirier, M.; Royo, G.; Young, J. C.; Belin, C. *J. Organomet. Chem.* **1994**, *470*, 43.
(20) Klebe, G. *J. Organomet. Chem.* **1987**, *332*, 35.
(21) Tamao, K.; Asahara, M.; Saeki, T.; Feng, S.; Kawachi, A.; Toshimitsu, A. *Chem. Lett.* **2000**, 660.
(22) Timosheva, N. V.; Chandrasekaran, A.; Day, R. O.; Holmes, R. R. *J. Am. Chem. Soc.* **2002**, *124*, 7035.
(23) Tamao, K.; Hayashi, T.; Ito, Y.; Shiro, M. *Organometallics* **1992**, *11*, 2099.
(24) Kano, N.; Kikuchi, A.; Kawashima, T. *Chem. Commun.* **2001**, 2096.
(25) Toshimitsu, A.; Hirao, S.; Saeki, T.; Asahara, M.; Tamao, K. *Heteroat. Chem.* **2001**, *12*, 392.

Table 2. Crystallographic Data for (*E*)-**2c**, (*E*)-**2f**, (*E*,*E*)-**3a**, (*E*)-**4d**, (*E*)-**4f**, (*E*)-**4g**, (*Z*)-**4f**, (*E*)-**5**, and (*Z*)-**5**

	(*E*)-**2c**	(*E*)-**2f**[a]	(*E*,*E*)-**3a**	(*E*)-**4d**	(*E*)-**4f**	(*E*)-**4g**	(*Z*)-**4f**	(*E*)-**5**[b]	(*Z*)-**5**[b]
empirical formula	$C_{25}H_{22}N_2Si$	$C_{24}H_{20}N_2Si$	$C_{26}H_{24}N_4Si$	$C_{12}H_9F_3N_2Si$	$C_{24}H_{19}FN_2Si$	$C_{18}H_{14}F_2N_2Si$	$C_{24}H_{19}FN_2Si$	$C_{24}H_{33}F_4KN_2O_6Si$	$C_{24}H_{33}F_4KN_2O_6Si$
formula wt	378.54	364.51	420.58	266.30	382.50	324.40	382.50	588.71	588.71
temp (K)	120(2)	120(2)	120(2)	293(2)	120(2)	120(2)	120(2)	120(2)	103(2)
crystal system	triclinic	triclinic	monoclinic	triclinic	triclinic	triclinic	monoclinic	orthorhombic	triclinic
space group	$P\bar{1}$	$P\bar{1}$	$P21/c$	$P\bar{1}$	$P\bar{1}$	$P\bar{1}$	$P21/c$	$P2_12_12_1$	$P\bar{1}$
a (Å)	9.940(6)	10.4650(14)	12.344(3)	8.235(6)	8.656(7)	8.502(6)	13.309(4)	9.314(3)	13.4452(17)
b (Å)	12.243(8)	10.7808(17)	9.256(2)	8.5166(6)	9.738(9)	9.120(7)	9.647(3)	16.258(6)	14.836(2)
c (Å)	17.692(11)	11.1487(11)	20.452(5)	9.2310(6)	13.170(11)	11.061(8)	15.468(5)	18.099(7)	15.750(2)
α (deg)	103.468(8)	91.788(2)	90	78.244(7)	101.156(8)	105.729(8)	90	90	74.096(6)
β (deg)	90.715(7)	114.662(3)	105.2130(13)	70.599(6)	99.258(8)	107.023(8)	101.5780(16)	90	69.804(3)
γ (deg)	102.807(8)	117.112(3)	90	85.024(3)	113.120(9)	93.714(7)	90	90	79.731(2)
V (Å^3)	2037(2)	978.6(2)	2254.9(9)	597.71(19)	966.6(14)	779.6(10)	1945.7(11)	2740.7(17)	2823.5(6)
Z	4	2	4	2	2	2	4	4	4
D_{calcd} (Mg/m^3)	1.234	1.237	1.239	1.480	1.314	1.382	1.306	1.427	1.385
abs coeff (mm^{-1})	0.128	0.130	0.125	0.217	0.142	0.171	0.142	0.306	0.297
F(000)	800	384	888	272	400	336	800	1232	1232
cryst size (mm^3)	0.6 × 0.45 × 0.1	0.6 × 0.45 × 0.2	0.40 × 0.35 × 0.3	0.6 × 0.4 × 0.15	0.4 × 0.25 × 0.1	0.35 × 0.25 × 0.05	0.5 × 0.45 × 0.4	0.6 × 0.55 × 0.35	0.5 × 0.30 × 0.05
θ range for data collection (deg)	3.04−25.00	3.43−25.00	3.01−25.00	2.44−25.00	3.12−25.00	3.18−25.00	3.09−25.00	3.14−25.00	2.23−25.00
index ranges	$-11 \le h \le 11$, $-12 \le k \le 14$, $-16 \le l \le 21$	$-12 \le h \le 10$, $-12 \le k \le 10$, $-13 \le l \le 13$	$-14 \le h \le 14$, $-10 \le k \le 10$, $-24 \le l \le 22$	$-9 \le h \le 9$, $-9 \le k \le 10$, $-10 \le l \le 10$	$-8 \le h \le 10$, $-11 \le k \le 11$, $-15 \le l \le 15$	$-10 \le h \le 8$, $-10 \le k \le 10$, $-11 \le l \le 13$	$-15 \le h \le 11$, $-11 \le k \le 11$, $-18 \le l \le 16$	$-10 \le h \le 11$, $-19 \le k \le 18$, $-21 \le l \le 21$	$-15 \le h \le 15$, $-14 \le k \le 17$, $-18 \le l \le 16$
reflections collected/ independent reflections	13 084/6955 [R(int) = 0.0162]	3333/6216 [R(int) = 0.0103]	13 525/3949 [R(int) = 0.0170]	4782/2022 [R(int) = 0.0223]	6173/3329 [R(int) = 0.0167]	4999/2659 [R(int) = 0.0150]	12 040/3370 [R(int) = 0.0193]	17 408/4787 [R(int) = 0.0213]	23 868/9794 [R(int) = 0.0449]
completeness to theta$_{max}$	96.9%	96.7%	99.2%	96.4%	97.3%	97.1%	98.0%	99.4%	98.6%
no. of parameters	507	247	282	163	253	208	253	343	685
goodness of fit on F^2	1.053	1.069	1.075	1.042	0.998	1.044	1.177	1.077	1.040
final R indices ($I > 2\sigma(I)$)	$R1 = 0.0347$, w$R2 = 0.0913$	$R1 = 0.0304$, w$R2 = 0.0751$	$R1 = 0.0340$, w$R2 = 0.0934$	$R1 = 0.0355$, w$R2 = 0.0980$	$R1 = 0.0367$, w$R2 = 0.0893$	$R1 = 0.0312$, w$R2 = 0.0790$	$R1 = 0.0368$, w$R2 = 0.0930$	$R1 = 0.0216$, w$R2 = 0.0551$	$R1 = 0.0678$, w$R2 = 0.1551$
R indices (all data)	$R1 = 0.0393$, w$R2 = 0.0978$	$R1 = 0.0330$, w$R2 = 0.0766$	$R1 = 0.0374$, w$R2 = 0.0962$	$R1 = 0.0448$, w$R2 = 0.1034$	$R1 = 0.0465$, w$R2 = 0.0962$	$R1 = 0.0394$, w$R2 = 0.0838$	$R1 = 0.0411$, w$R2 = 0.0964$	$R1 = 0.222$, w$R2 = 0.0557$	$R1 = 0.1115$, w$R2 = 0.1803$
largest diff peak and hole (e Å^{-3})	0.294 and −0.270	0.313 and −0.241	0.276 and −0.283	0.210 and −0.179	0.327 and −0.277	0.272 and −0.0263	0.330 and −0.278	0.209 and −0.193	1.046 and −0.451

[a] Reference 11. [b] Reference 9.

Table 3. Selected Bond Lengths (Å) and Bond Angles (deg) for (*E*)-**2c**, (*E*)-**2f**, (*E*,*E*)-**3a**, (*E*)-**4d**, (*E*)-**4f**, (*E*)-**4g**, (*Z*)-**4f**, (*E*)-**5**, and (*Z*)-**5**

				(*E*)-**2c**			
Si1−C1	1.8899(18)	Si2−C38	1.8688(19)	C1−Si1−C13	111.97(7)	C26−Si2−C38	112.09(7)
Si1−C13	1.8651(19)	Si2−C39	1.8771(18)	C1−Si1−C14	110.46(7)	C26−Si2−C39	110.64(7)
Si1−C14	1.8786(18)	Si2−C45	1.8821(17)	C1−Si1−C20	106.47(7)	C26−Si2−C45	107.66(7)
Si1−C20	1.8803(17)	N1−N2	1.2564(18)	C13−Si1−C14	110.50(7)	C38−Si2−C39	109.70(7)
Si2−C26	1.8854(19)	N3−N4	1.2580(18)	C13−Si1−C20	108.71(7)	C38−Si2−C45	107.87(8)
				C14−Si1−C20	108.58(8)	C39−Si2−C45	108.77(7)
				(*E*)-**2f**[a]			
Si1−C1	1.8757(13)	Si1−H1	1.397(13)	C1−Si1−C13	110.93(6)	C1−Si1−H1	111.4(6)
Si1−C13	1.8712(13)	N1−N2	1.2546(15)	C1−Si1−C19	108.94(6)	C13−Si1−H1	110.2(6)
Si1−C19	1.8741(13)			C13−Si1−C19	109.83(6)	C19−Si1−H1	105.5(6)
				(*E*,*E*)-**3a**			
Si1−C1	1.8899(14)	Si1−C26	1.8649(14)	C1−Si1−C13	108.16(6)	C13−Si1−C25	110.45(6)
Si1−C13	1.8906(14)	N1−N2	1.2515(16)	C1−Si1−C25	111.47(6)	C13−Si1−C26	106.47(7)
Si1−C25	1.8671(13)	N3−N4	1.2548(16)	C1−Si1−C26	109.64(6)	C25−Si1−C26	110.50(6)
				(*E*)-**4d**			
Si1−C1	1.8433(18)	Si1−F3	1.5720(12)	C1−Si1−F1	100.62(7)	F2−Si1−F3	111.61(7)
Si1−F1	1.5991(12)	N1−N2	1.2589(18)	C1−Si1−F2	120.19(7)	C1−Si1···N2	76.21(6)
Si1−F2	1.5750(13)	Si1···N2	2.3030(14)	C1−Si1−F3	120.47(8)	F1−Si1···N2	176.62(6)
				F1−Si1−F2	98.59(7)	F2−Si1···N2	82.17(6)
				F1−Si1−F3	98.58(7)	F3−Si1···N2	84.15(6)
				(*E*)-**4f**			
Si1−C1	1.871(2)	Si1−F1	1.6343(17)	C1−Si1−C13	116.36(9)	C19−Si1−F1	99.49(7)
Si1−C13	1.857(2)	N1−N2	1.263(2)	C1−Si1−C19	118.87(9)	C1−Si1···N2	71.21(6)
Si1−C19	1.860(2)	Si1···N2	2.605(2)	C13−Si1−C19	117.13(8)	C13−Si1···N2	84.77(6)
				C1−Si1−F1	99.10(7)	C19−Si1···N2	86.40(7)
				C13−Si1−F1	99.21(6)	F1−Si1···N2	170.27(5)
				(*E*)-**4g**			
Si1−C1	1.854(2)	Si1−F2	1.5931(12)	C1−Si1−C13	117.16(7)	F1−Si1−F2	97.65(6)
Si1−C13	1.850(2)	N1−N2	1.2594(19)	C1−Si1−F1	99.65(6)	C1−Si1···N2	73.99(6)
Si1−F1	1.6201(14)	Si1···N2	2.419(2)	C1−Si1−F2	120.49(7)	C13−Si1···N2	83.07(6)
				C13−Si1−F1	103.14(7)	F1−Si1···N2	172.78(5)
				C13−Si1−F2	113.29(8)	F2−Si1···N2	83.03(6)
				(*Z*)-**4f**			
Si1−C1	1.8698(17)	Si1−F1	1.6190(12)	C1−Si1−C13	120.40(7)	C1−Si1−F1	102.28(7)
Si1−C13	1.8597(18)	N1−N2	1.255(2)	C1−Si1−C19	108.70(8)	C13−Si1−F1	103.45(7)
Si1−C19	1.8600(17)			C13−Si1−C19	114.29(7)	C19−Si1−F1	105.80(6)
				(*E*)-**5**[b]			
Si1−C1	1.9120(15)	Si1−F4	1.6597(9)	C1−Si1−F1	99.47(6)	F2−Si1−F4	88.69(5)
Si1−F1	1.6428(10)	N1−N2	1.2581(17)	C1−Si1−F2	90.62(6)	F3−Si1−F4	87.63(5)
Si1−F2	1.6661(10)	Si1···N2	2.2498(13)	C1−Si1−F3	90.10(6)	C1−Si1···N2	76.41(6)
Si1−F3	1.6923(9)			C1−Si1−F4	164.73(6)	F1−Si1···N2	175.65(5)
				F1−Si1−F2	96.93(5)	F2−Si1···N2	84.58(5)
				F1−Si1−F3	94.12(5)	F3−Si1···N2	84.57(5)
				F1−Si1−F4	95.76(5)	F4−Si1···N2	88.34(5)
				F2−Si1−F3	168.65(5)		
				(*Z*)-**5**[b]			
Si1−C1	1.890(5)	Si2−C25	1.872(4)	C1−Si1−F1	117.77(19)	C25−Si2−F5	117.73(19)
Si1−F1	1.617(3)	Si2−F5	1.607(3)	C1−Si1−F2	91.16(17)	C25−Si2−F6	91.28(17)
Si1−F2	1.668(3)	Si2−F6	1.676(3)	C1−Si1−F3	90.53(17)	C25−Si2−F7	91.08(17)
Si1−F3	1.697(3)	Si2−F7	1.681(3)	C1−Si1−F4	126.67(19)	C25−Si2−F8	122.51(19)
Si1−F4	1.611(3)	Si2−F8	1.622(3)	F1−Si1−F2	90.29(16)	F5−Si2−F6	90.24(19)
N1−N2	1.261(5)	N3−N4	1.250(5)	F1−Si1−F3	88.88(15)	F5−Si2−F7	89.93(17)
				F1−Si1−F4	115.53(16)	F5−Si2−F8	119.75(17)
				F2−Si1−F3	178.31(16)	F6−Si2−F7	177.23(16)
				F2−Si1−F4	90.26(16)	F6−Si2−F8	89.25(16)
				F3−Si1−F4	88.77(16)	F7−Si2−F8	88.25(15)

[a] Reference 11. [b] Reference 9.

while those of the fluorosilanes (*E*)-**4d**, (*E*)-**4f**, and (*E*)-**4g** [1.2589(18)−1.263(2)Å] tend to be slightly longer than those of the (*E*)-azobenzenes which have no Si···N interaction. Elongation of these N═N bonds indicates slight decrease of its double-bond character caused by the coordination of the lone pairs to the silicon atoms.

UV−vis Spectral Properties

The absorption maxima in the UV−vis spectra of (*E*)-**2a**−**g**, (*E*,*E*)-**3a**−**d**, and (*E*)-**4d**−**g** in CH_2Cl_2 due to their $\pi-\pi^*$ and $n-\pi^*$ transitions are summarized in Table 1. The absorption maxima due to the 2-silylazobenzenes were expected to shift from that of the unsubstituted azobenzene because the electropositive silyl substituents should perturb both $\pi-\pi^*$ and $n-\pi^*$ transitions. Actually, 2-silylazobenzenes (*E*)-**2a**−**g** and (*E*,*E*)-**3a**−**d** showed their absorption maxima of $\pi-\pi^*$ and $n-\pi^*$ transitions at 325−327 and 441−456 nm, respectively, in CH_2-

(26) Allman, R. In *The Chemistry of the Hydrazo, Azo and Azoxy Groups, Part 1*; Patai, S., Ed.; John Wiley & Sons: New York, 1975; pp 41−48.
(27) Harada, J.; Ogawa, K.; Tomoda, S. *Acta Crystallogr., Sect. B* **1997**, *53*, 662.

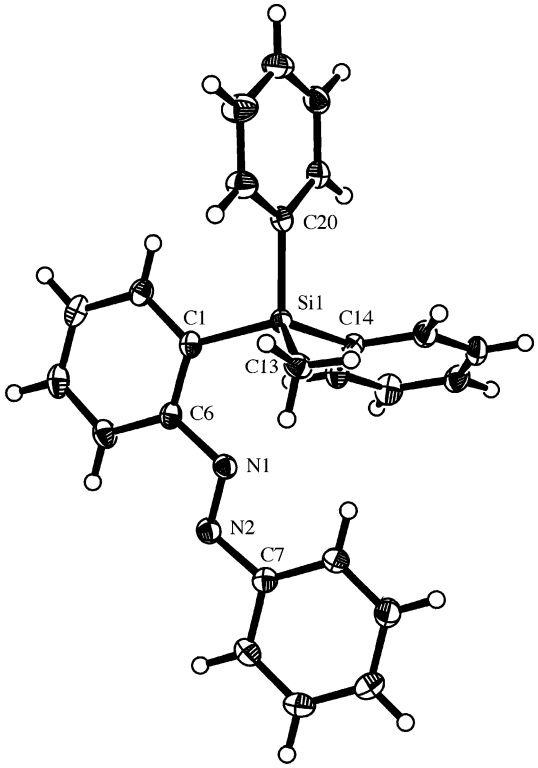

Figure 1. ORTEP drawing of (*E*)-**2c** (50% probability). One of two independent molecules in the crystal is shown.

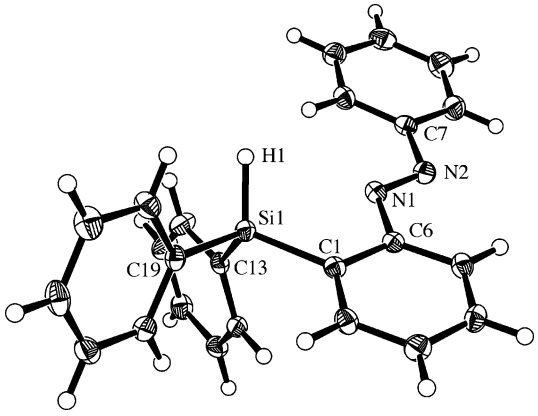

Figure 2. ORTEP drawing of (*E*)-**2f** (50% probability).

Cl_2. Both the $\pi-\pi^*$ and $n-\pi^*$ transitions showed slight red-shifts from those of the unsubstituted azobenzene ($\pi-\pi^*$ transition, 318 nm; $n-\pi^*$ transition, 441 nm). The n and π orbitals should be destabilized by the inductive effect of the electron-donating silyl groups. The color of the solutions is red similarly to the unsubstituted azobenzene, indicating a relatively small perturbation caused by the silyl groups.

By contrast, the color of fluorosilanes (*E*)-**4d**−**g** is yellow, suggesting a considerable perturbation of the electronic structure of the azo unit. In the UV−vis spectra in CH_2Cl_2, they showed a red shift of the $\pi-\pi^*$ transition and a blue shift of the $n-\pi^*$ transition from those of the unsubstituted azobenzene. The red-shifted $\pi-\pi^*$ transitions of the difluorosilane (*E*)-**4g** and trifluorosilane (*E*)-**4d** overlapped with $n-\pi^*$ transitions, which could not be identified. The wavelengths of their $n-\pi^*$ transitions can be estimated to be shorter than those of monofluorosilanes (*E*)-**4e** and (*E*)-**4f**. The wavelengths of absorption maxima of the $\pi-\pi^*$ transitions of (*E*)-**4g** and (*E*)-

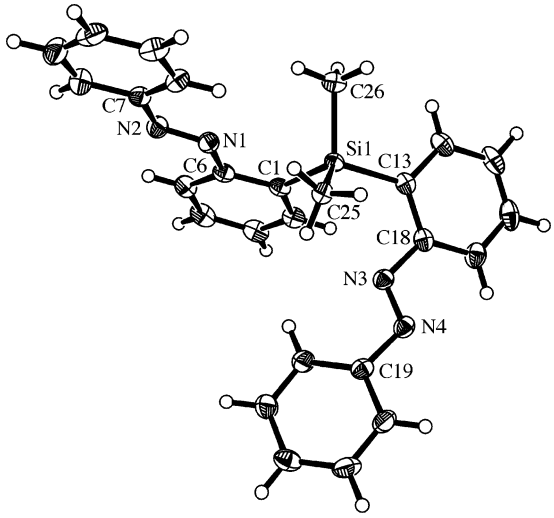

Figure 3. ORTEP drawing of (*E*,*E*)-**3a** (50% probability).

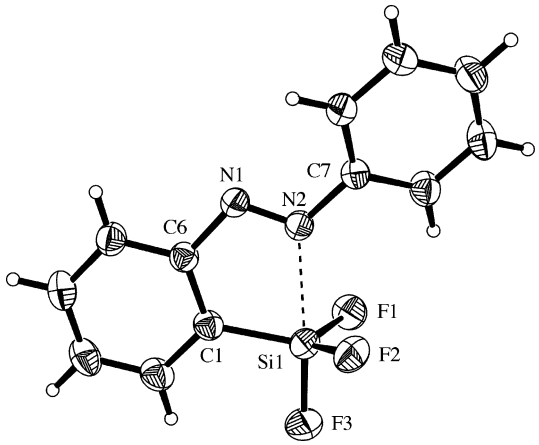

Figure 4. ORTEP drawing of (*E*)-**4d** (30% probability).

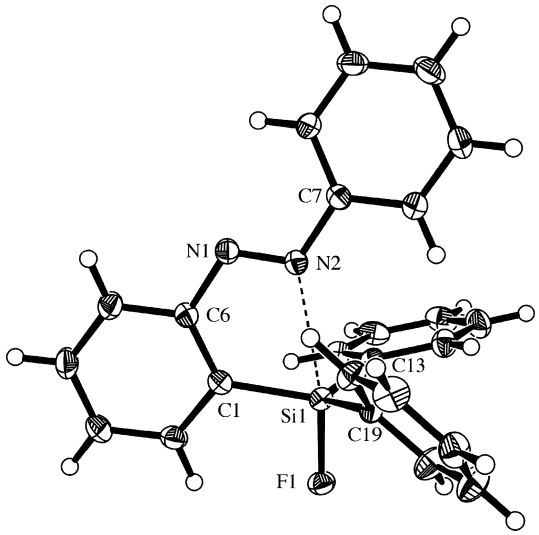

Figure 5. ORTEP drawing of (*E*)-**4f** (50% probability).

4d are longer than those of monofluorosilanes (*E*)-**4e** and (*E*)-**4f**, while those of their $n-\pi^*$ transitions are in the reverse order, considering their overlap as described above. These spectral features are explained by the Si···N interaction. The n orbital (lone pair of the nitrogen atom) is stabilized significantly by its donation to the silicon atom. The π and π^* orbitals are less stabilized by the Si−N interaction than the n orbital; what is

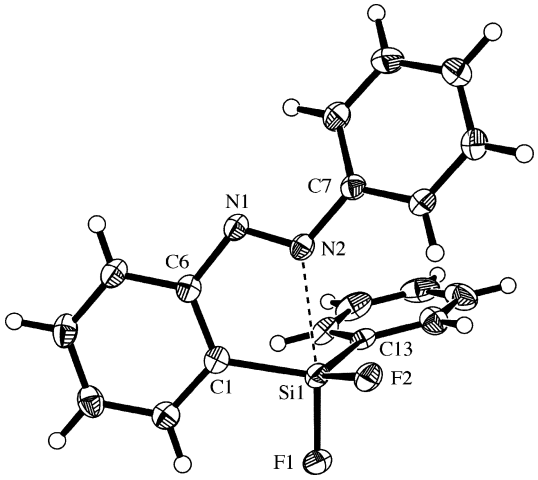

Figure 6. ORTEP drawing of (*E*)-**4g** (50% probability).

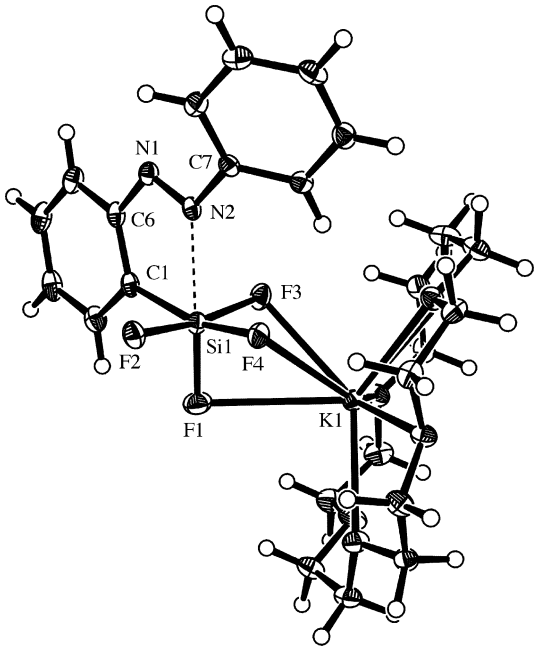

Figure 7. ORTEP drawing of (*E*)-**5** (50% probability).

more, the π orbital is less stabilized than the π^* orbital. The greater the number of the fluorine atoms, the more these orbitals are stabilized and the longer the wavelength of the absorption maxima shift.

In the UV−vis spectra of (*E*)-**5**, an absorption maximum due to $\pi-\pi^*$ transition of the azo group was observed at 334 nm in CH_2Cl_2. The red shift of the absorption maximum is explained by the above discussion, considering its overlap with the $n-\pi^*$ transition.

Isomerization of Azobenzenes Bearing a Fluorosilyl Substituent

In the (*Z*)-isomers of the fluorosilanes bearing an azobenzene unit, the silicon atom is expected to have a tetracoordination state without the Si−N interaction. To achieve the photoswitching of the coordination numbers of the silicon atom, photoisomerization of the azobenzene moiety of the pentacoordinate fluorosilanes was carried out. A CH_2Cl_2 solution of (*E*)-**4f** (λ_{max} = 336 nm in CH_2Cl_2) was irradiated with a high-pressure Hg-lamp (λ = 360 nm) fitted with a colored-glass filter, which was

Scheme 5

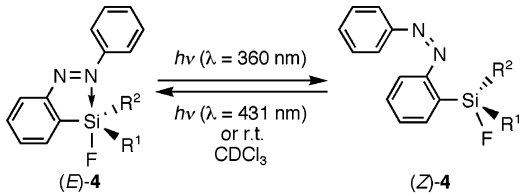

	Ratio of (*E*)/(*Z*)	
compounds	λ = 360 nm	λ = 431 nm
4d	19/81	100/0
4e	1/99	83/17
4f	2/98	83/17
4g	1/99	83/17

used to limit the wavelengths, for 1 h to give (*Z*)-**4f** (Scheme 5). When the photoisomerization of (*E*)-**4f** was monitored by the UV−vis spectra, the absorption maximum at 336 nm of the $\pi-\pi^*$ transition of the azo group decreased, and a new absorption maximum at 445 nm assignable to the $n-\pi^*$ transition of (*Z*)-**4f** increased (Figure 8). The absorption maximum is almost the same as that of the (*Z*)-isomer of unsubstituted azobenzene. Irradiation (λ = 431 nm) of (*Z*)-**4f** caused regeneration of (*E*)-**4f**.

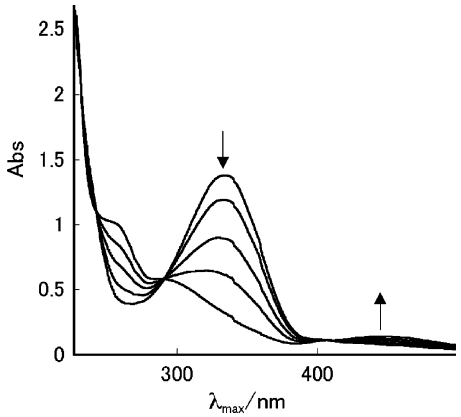

Figure 8. UV/vis spectra of the CH_2Cl_2 solution of (*E*)-**4f** irradiated with high pressure Hg lamp (λ_{max} = 360 nm). The spectra were recorded every 30 s.

The photoisomerization reactions of (*E*)- and (*Z*)-isomers of these 2-silylazobenzenes were monitored by the ^1H, ^{19}F, and ^{29}Si NMR spectra. In the ^{19}F NMR spectra in $CDCl_3$, the signal of (*E*)-**4f** (δ_F −152.1) decreased and a new singlet (δ_F −170.6), which was assigned to (*Z*)-**4f**, emerged and increased during irradiation of (*E*)-**4f**. The ratio of (*E*)-**4f**/(*Z*)-**4f** was estimated as 2:98 based on the integral of the ^{19}F NMR spectra of the reaction solution at the photostationary state. Similarly, in the ^1H NMR spectra in $CDCl_3$ the peaks of (*E*)-**4f** decreased and new peaks of its (*Z*)-isomers increased during the irradiation. Irradiation (λ = 431 nm) of (*Z*)-**4f** caused isomerization to (*E*)-**4f** in the ratio (*E*)-**4f**/(*Z*)-**4f** = 83:17 based on the integral of the ^{19}F NMR spectra. Such changes of the signals are in accordance with the behavior in the UV−vis spectra. In the ^{29}Si NMR spectra, a doublet of (*Z*)-**4f** resonated at δ_{Si} −7.3, which is almost the same chemical shift as that of fluorotriphenylsilane (δ_{Si} −4.7) and is much lower than that of pentacoordinate (*E*)-**4f** (δ_{Si} −16.3), suggesting a tetracoordinate structure around the silicon atom of (*Z*)-**4f** in the absence of coordination of nitrogen to silicon. That is, the coordination numbers of

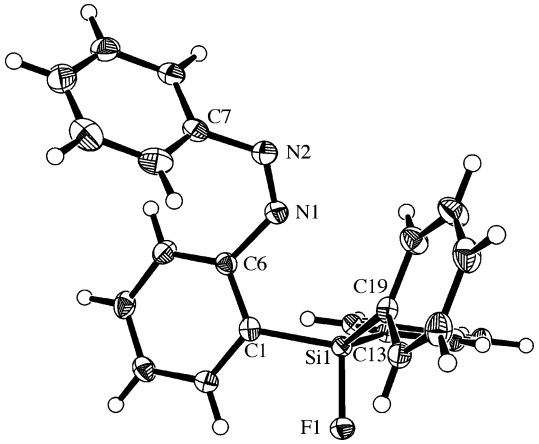

Figure 9. ORTEP drawing of (*Z*)-**4f** (50% probability).

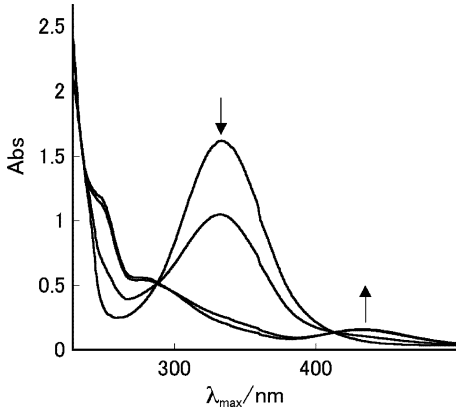

Figure 10. UV/vis spectra of the CH_2Cl_2 solution of (*E*)-**5** irradiated with high pressure Hg lamp (λ_{max} = 360 nm). The spectra were recorded every 30 s.

silicon are five in (*E*)-**4f** and four in (*Z*)-**4f**. Since (*E*)- and (*Z*)-**4f** are converted reversibly by photoirradiation, it can be said that the coordination number of silicon in the fluorosilane is switched reversibly by photoirradiation.

Photoisomerization (λ = 360 nm) of (*E*)-**4d**, (*E*)-**4e**, and (*E*)-**4g** occurred similarly to give the corresponding (*Z*)-isomers (Scheme 5). The ^{29}Si NMR chemical shifts of the (*Z*)-isomers are summarized in Table 1. Irradiation (λ = 431 nm) of the absorption maxima of the (*Z*)-isomers caused a decrease of the absorption maxima of the n−π* transitions and an increase of the $\pi-\pi$* transitions of the azo group of the (*E*)-isomers. Namely, the (*E*)-isomers were regenerated by the photoisomerization of the (*Z*)-isomers. The reversibility of the isomerization and the changes in the ^{29}Si chemical shifts show that the coordination number of the silicon atom in the fluorosilanes is switched reversibly by photoirradiation. Interestingly, the coordination state can visually be recognized with ease by the change of the color from yellow to red because the azo moiety works both as a chromophore and as a coordination site in the (*E*)-form. Photoirradiation of (*E*,*E*)-**3d**, which has two azobenzene moieties, resulted in the mixture of three isomers in the ratio (*E*,*E*)-**3d**/(*E*,*Z*)-**3d**/(*Z*,*Z*)-**3d** = 13:15:72 as judged by the integral of ^{19}F NMR spectra. Unfortunately, the signal due to neither (*E*,*Z*)-**3d** nor (*Z*,*Z*)-**3d** was observed in the ^{29}Si NMR spectrum.

In addition, in the ^{19}F NMR spectra at −70 °C, the peak of (*Z*)-**4d** was maintained as a singlet and did not split in contrast to that of (*E*)-**4d**. Furthermore, the higher the concentration of the solution of (*Z*)-**4d** was, the broader the signal became. These results suggest that the silicon atom has no interaction with the nitrogen atom and that the fluorine nuclei exchange both inter- and intramolecularly faster than the time scale of ^{19}F NMR spectroscopy even at −70 °C. Compound (*Z*)-**4d** is thermally more labile than (*Z*)-**4e**−**g**, and its complete thermal isomerization to the (*E*)-**4d** within 6 h upon standing at rt in the dark was confirmed by the UV−vis spectra.

A single crystal of (*Z*)-**4f** was obtained by recrystallization from hexane. The crystal structure of (*Z*)-**4f** was determined by the X-ray crystallographic analysis. Its crystallographic data and selected bond lengths (Å) and angles (deg) are summarized in Tables 2 and 3, respectively. The ORTEP drawing of (*Z*)-**4f** is shown in Figure 9. In (*Z*)-**4f**, the azobenzene moiety clearly shows a (*Z*)-form with a small C6−N1−N2−C7 torsion angle (5.4(2)°), while the corresponding torsion angle in (*E*)-**4f** is 178.05(13)°. The Si1−F1 bond length (1.6169(11) Å) is comparable to that of fluorotris(2-methylphenyl)silane (Si−F: 1.601(1) Å).[29] Structural changes between (*E*)-**4f** and (*Z*)-**4f** were found on the widening of the C_n−Si1−F1 (n = 1, 13, 19) bond angles (102.26(6)°−105.84(6)°) in (*Z*)-**4f** compared to those (99.10(7)°−99.49(7)°) in (*E*)-**4f** and shortening of the Si1−F1 bond length (1.6169(11) Å) in (*Z*)-**4f** compared to that (1.6343-(17) Å) in (*E*)-**4f**. In (*Z*)-**4f**, the N1−N2 bond length (1.252(2) Å) is almost the same as that of unsubstituted (*Z*)-azobenzene (1.253 Å).[30] In the crystalline state, the Si1 atom evidently lacks the interaction with the N2 atom and adopted a tetracoordination state with a distorted tetrahedral structure. The pentacoordination character values of (*Z*)-**4f** (%TBP_a, 29% and %TBP_e, 47%) are much lower than those of (*E*)-**4f** (%TBP_a, 53% and %TBP_e, 76%), respectively. The configuration of the aryl groups around the silicon atom of **4f** in the crystalline state has appreciably been changed from a distorted TBP structure to a tetrahedral structure by the photoisomerization.

The coordination number of the silicon atom of tetrafluorosilicate (*E*)-**5** can be converted from six to five by elimination of a fluoride ion induced by addition of a Lewis acid. Treatment of (*E*)-**5** with an excess amount of BF_3·OEt_2 gave the corresponding trifluorosilane (*E*)-**4d** and a tetrafluoroborate anion quantitatively within 5 min (Scheme 4). Furthermore, the coordination number of the silicon atom can also be changed by photoirradiation. Isomerization of (*E*)-**5** could easily be done by irradiation (λ = 360 nm) in CH_2Cl_2 for 40 min to give orange-colored (*Z*)-**5** (Figure 10).[9] (*Z*)-**5** showed its absorption maximum at 433 nm assignable to the n−π* transition. Irradiation (λ = 431 nm) of the new absorption maximum led to the recovery of (*E*)-**5** with a decrease of its absorption. In variable-temperature ^{19}F NMR spectra, the signal of (*Z*)-**5** was observed at δ_{Si} −114.7 as a broad singlet and did not split even at −70 °C in contrast to that of (*E*)-**5**. The ratio of (*E*)-**5**/(*Z*)-**5** is estimated as 2:98 by the integral of ^{19}F NMR spectra of the reaction solution after irradiation for 40 min. Furthermore, the higher concentration of the solution of (*Z*)-**5** was, the broader the signal became, suggesting the intermolecular fluorine exchange. The ^{29}Si NMR spectra of (*Z*)-**5** at −65 °C showed a quintet at δ_{Si} −122.8, which is lower field by 28 ppm than that

(28) Birnbaum, P. P.; Linford, J. H.; Style, D. W. G. *Trans. Faraday Soc.* **1953**, *49*, 735.
(29) Dell, S.; Ho, D. M.; Pascal, R. A., Jr. *J. Org. Chem.* **1999**, *64*, 5626.
(30) Mostad, A.; Rømming, C. *Acta Chem. Scand.* **1971**, *25*, 3561.

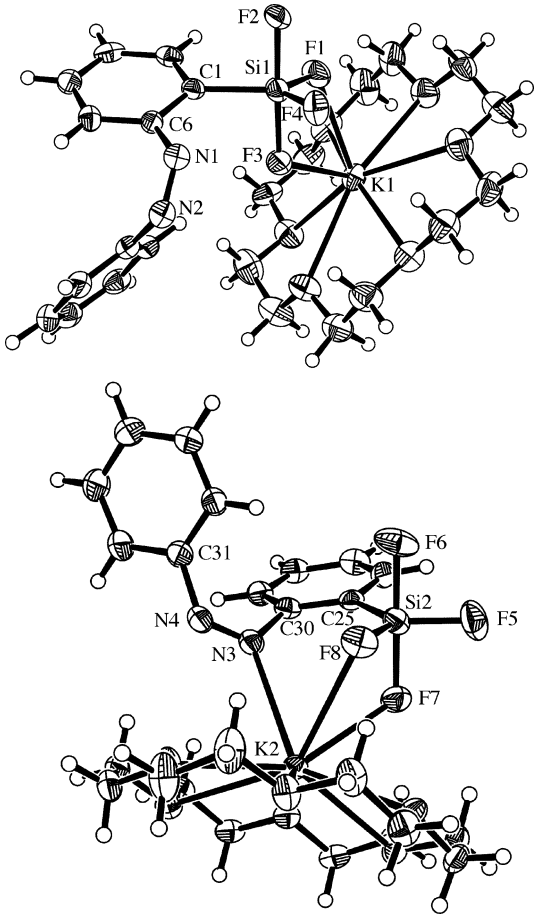

Figure 11. ORTEP drawings of two independent isomers of (*Z*)-**5** (50% probability).

of (*E*)-**5**. These results suggest that fluorine nuclei exchange faster than the time scale of ^{19}F NMR spectroscopy even at −65 °C both intra- and intermolecularly and that (*Z*)-**5** bears a pentacoordinate structure around a silicon atom in the absence of coordination of the nitrogen atom. Addition of BF_3·OEt_2 to (*Z*)-**5** caused both elimination of a fluoride ion and isomerization of the azo moiety to give the corresponding trifluorosilane (*E*)-**4d** quantitatively within 5 min.

The (*Z*)-**5** is stable under argon at ambient temperature for a few days in the solid state, and it gradually isomerizes to (*E*)-**5** at room temperature in solution state even in the dark. The crystal structure of (*Z*)-**5** was finally determined by X-ray crystallographic analysis (Figure 11).[9] There are two nonidentical molecules (molecules 1 and 2) of (*Z*)-**5** in the unit cell, and they have a similar conformation around the silicon atom. In (*Z*)-**5**, the silicon atom evidently lacked the Si1−N2 interaction and adopted a pentacoordinate state of a TBP structure with F2 and F3 atoms at apical positions and with F1, F4, and C1 atoms at equatorial positions. The pentacoordination characters, $\%TBP_a$ and $\%TBP_e$, are 97% and 100%, respectively. The deviation from an ideal TBP structure to a square pyramidal structure, TBP→SP, was calculated to be 22%.[31] The bond lengths of Si1−F2 (1.668(3) Å) and Si1−F3 (1.697(3) Å) bonds are significantly longer than those of Si1−F1 (1.617(3) Å) and Si1−F4 (1.611(3) Å) bonds. Such elongation of apical bonds is indeed characteristic of TBP structure around a pentacoordinate silicon atom. Structural changes between (*E*)-**5** and (*Z*)-**5** were found on the widening of the bond angles of C1−Si1−F4 (164.73(6)°) and the narrowing of F1−Si1−F4 (95.76(5)°) and C1−Si1−F1 (99.47(6)°) in (*E*)-**5** compared to those of (*Z*)-**5** (126.67(19)°, 115.53(16)°, and 117.77(19)°, respectively). The changes in the bond angles between (*E*)-**5** and (*Z*)-**5** are more remarkable than the changes between (*E*)-**4f** and (*Z*)-**4f**. Configuration around the silicon atom in **5** has completely been changed between distorted octahedral and TBP structures by photoirradiation. Such a change around the silicon atom by irradiation has never been reported as far as we know.

In the previous reports of the photoswitching by taking advantage of the photoisomerization of azobenzenes, the azobenzenes were substituted at the 4- and 4′-positions or the 3- and 3′-positions.[7] The differences in the directions of two C(*ipso*)−N(azo) bonds and the relative location of the substituents between the (*E*)- and (*Z*)-isomers were utilized for the photoswitching. In contrast with the previous reports, location and direction of the lone pair of the nitrogen atom that coordinates to the silicon atom are important for our photoswitching of the coordination numbers of the silicon. The switching is achieved by change of the relative location of the lone pair of the nitrogen and the silicon atom. If the silicon atom is located on the other side of the lone pair, such a photoswitching cannot be achieved. The configuration of the lone pair of the nitrogen atom in the (*Z*)-isomers is too far away from the silicon to coordinate, while the lone pair is close enough to the silicon atom in the (*E*)-form.

Concluding Remarks

We have synthesized several neutral pentacoordinate organosilicon compounds bearing one or two 2-(phenylazo)phenyl groups. They have been characterized by ^{1}H, ^{13}C, ^{19}F, and ^{29}Si NMR spectroscopy, UV−vis spectroscopy, and X-ray crystallographic analyses. The spectral properties depending on the coordination numbers are exposed in the chemical shifts and the coupling patterns in the ^{19}F and ^{29}Si NMR spectra. The silicon atom of the silanes bearing no fluorine atom has a tetracoordinate structure, while that of the (*E*)-isomers of the fluorosilanes bearing at least one fluorine atom has a pentacoordinate structure in both the solution state and the crystalline state. In the tetracoordinate silanes, the silyl group causes the red shifts of the n−π* and π−π* transitions of the azo groups compared to the unsubstituted azobenzene in the UV−vis spectra. The (*E*)-isomers of the fluorosilanes show the intramolecular electron-pair donation from a nitrogen atom of the azo group to the silicon atom and exhibited distorted TBP geometry around the pentacoordinate silicon atom. The photoirradiation of the (*E*)-isomers of fluorosilanes reversibly gives the corresponding (*Z*)-isomers in good yields. The (*Z*)-isomers have been found to have a tetracoordinate silicon atom in the absence of the Si···N interaction. We have achieved reversible photocontrol of the coordination numbers of the silicon atom of the fluorosilanes between four and five as well as that of the silicate between five and six.

Experimental Section

General Procedure. Solvents were purified before use by reported methods. All reactions were carried out under argon atmosphere unless otherwise noted. The ^{1}H NMR (500 MHz),

(31) Holmes, R. R.; Deiters, J. A. *J. Am. Chem. Soc.* **1977**, *99*, 3318.

^{13}C NMR (125 MHz), and ^{29}Si NMR (99 MHz) spectra were measured with a JEOL A500 spectrometer using tetramethylsilane (TMS) as an internal standard. The ^{19}F NMR (254 MHz) and ^{19}F NMR (376 MHz) spectra were measured with a JEOL EXcalibur270 spectrometer and a JEOL AL400 spectrometer, respectively, using Fleon as an external standard. All melting points are uncorrected. FAB-Mass and EI-Mass spectral data were obtained on a JEOL JMS-SX102 spectrometer. Preparative gel permeation liquid chromatography was performed by LC-918 with JAIGEL H1 + H2 columns (Japan Analytical Industry) with chloroform as the solvent. Elemental analyses were performed by the Microanalytical Laboratory of Department of Chemistry, Faculty of Science, The University of Tokyo. 2-Bromoazobenzene and 2-iodoazobenzene were prepared according to literature.[32]

Preparation of 2-(Phenylazo)phenyllithium. To a THF solution (12.5 mL) of 2-iodoazobenzene (**1b**) (500 mg, 1.62 mmol) at −105 °C, *n*-BuLi (1.50 M in hexane, 1.11 mL, 1.67 mmol) was added rapidly. After the reaction solution was stirred further at −105 °C for 5 min, the black solution of 2-lithioazobenzene was used at −105 °C for the syntheses of (*E*)-**2a**−**g** and (*E*,*E*)-**3a**−**c**.

A General Procedure for the Synthesis of [2-((*E*)-Phenylazo)phenyl]silanes ((*E*)-2a−g) and Bis[2-((*E*)-phenylazo)-phenyl]silanes (*E*,*E*)-3a−c. To a THF solution (12.5 mL) of 2-lithioazobenzene (1.70 mmol) at −105 °C was added a chlorosilane (1.79 mmol) for the synthesis of (*E*)-**2** or a dichlorosilane (0.88 mmol) for the synthesis of (*E*,*E*)-**3**. The reaction mixture was stirred at 0 °C for 3 h and quenched with aq. $NaHCO_3$. After separation of the organic layer, extraction of the aqueous layer with $CHCl_3$, drying of the combined solution with $MgSO_4$, and evaporation of the solvent, the residue was separated with alumina-gel column chromatography. A red-colored fraction was collected, and the eluent was evaporated. For oil compounds, the products were used as such for the next reactions, and further purification with gel permeation liquid chromatography gave analytically pure products. For crystalline compounds, recrystallization gave pure products. The yields of (*E*)-**2a**−**g** and (*E*,*E*)-**3a**−**c** are summarized in Scheme 2.

Spectral and Physical Data of (*E*)-2a−g. Trimethyl[2-((*E*)-phenylazo)phenyl]silane ((*E*)-2a): Red oil. ^{1}H NMR (500 MHz, $CDCl_3$) δ 0.38 (s, 9H), 7.43 (dt, $^3J_{HH}$ = 7.5 Hz, $^4J_{HH}$ = 1.5 Hz, 1H), 7.45−7.49 (m, 2H), 7.53 (t, $^3J_{HH}$ = 7.5 Hz, 2H), 7.69 (dd, $^3J_{HH}$ = 7.5 Hz, $^4J_{HH}$ = 1.5 Hz, 1H), 7.75 (dd, $^3J_{HH}$ = 7.5 Hz, $^4J_{HH}$ = 1.5 Hz, 1H), 7.92 (d, $^3J_{HH}$ = 7.5 Hz, 2H). ^{13}C NMR (125 MHz, $CDCl_3$) δ 0.52 (q), 114.84 (d), 123.18 (d), 129.15 (d), 129.94 (d), 130.06 (d), 130.89 (d), 134.73 (d), 141.77 (s), 152.59 (s), 157.42 (s). ^{29}Si NMR (53 MHz, $CDCl_3$) δ −3.98 (s). HRMS (EI, 70 eV) *m*/*z* Calcd for $C_{15}H_{18}N_2Si$: 254.1239. Found: 254.1243. Anal. Calcd for $C_{15}H_{18}N_2Si$: C, 70.82; H, 7.13; N, 11.01. Found: C, 70.67; H, 6.97; N, 10.98%.

Dimethylphenyl[2-((*E*)-phenylazo)phenyl]silane ((*E*)-2b): Orange needles (ethanol), mp 110−111 °C. ^{1}H NMR (500 MHz, $CDCl_3$) δ 0.63 (s, 6H), 7.29−7.35 (m, 3H), 7.39−7.46 (m, 4H), 7.49 (dt, $^3J_{HH}$ = 7.5 Hz, $^4J_{HH}$ = 1.5 Hz, 1H), 7.54−7.58 (m, 3H), 7.66−7.68 (m, 2H), 7.76 (d, $^3J_{HH}$ = 7.5 Hz, 1H). ^{13}C NMR (126 MHz, $CDCl_3$) δ −0.56 (q), 114.94 (d), 123.15 (d), 127.65 (d), 128.75 (d), 128.97 (d), 130.13 (d), 130.33 (d), 130.80 (d), 134.17 (d), 135.94 (d), 139.22 (s), 139.84 (s), 152.54 (s), 157.34 (s). ^{29}Si NMR (99 MHz, $CDCl_3$) δ −7.53 (s). Anal. Calcd for $C_{20}H_{20}N_2Si$: C, 75.90; H, 6.37; N, 8.85. Found: C, 75.67; H, 6.39; N, 8.95%.

Methyldiphenyl[2-((*E*)-phenylazo)phenyl]silane ((*E*)-2c): Orange needles (ethanol), mp 115−116 °C. ^{1}H NMR (500 MHz, $CDCl_3$) δ 0.88 (s, 3H), 7.27−7.36 (m, 11H), 7.38 (dt, $^3J_{HH}$ = 7.5 Hz, $^4J_{HH}$ = 1.5 Hz, 1H), 7.43 (dd, $^3J_{HH}$ = 7.5 Hz, $^4J_{HH}$ = 1.5 Hz, 1H), 7.51−7.54 (m, 5H), 7.82 (dd, $^3J_{HH}$ = 7.5 Hz, $^4J_{HH}$ = 1.5 Hz, 1H). ^{13}C NMR (126 MHz, $CDCl_3$) δ −1.45 (q), 115.08 (d), 123.11 (d), 127.69 (d), 128.76 (d), 128.95 (d), 130.24 (d), 130.65 (d), 130.68 (d), 135.13 (d), 137.33 (s), 137.35 (d), 138.14 (s), 152.49 (s), 157.18 (s). ^{29}Si NMR (53 MHz, $CDCl_3$) δ −10.29 (s). Anal. Calcd for $C_{25}H_{22}N_2Si$: C, 79.32; H, 5.86; N, 7.40. Found: C, 79.17; H, 5.98; N, 7.53%.

Triethoxy[2-((*E*)-phenylazo)phenyl]silane ((*E*)-2d): Red oil. ^{1}H NMR (500 MHz, $CDCl_3$) δ 1.18 (t, $^3J_{HH}$ = 7.0 Hz, 9H), 3.86 (q, $^3J_{HH}$ = 7.0 Hz, 6H), 7.45−7.56 (m, 5H), 7.81 (d, $^3J_{HH}$ = 8.0 Hz, 1H), 8.01−8.03 (m, 3H). ^{13}C NMR (126 MHz, $CDCl_3$) δ 18.13 (q), 58.62 (t), 114.92 (d), 123.35 (d), 129.03 (d), 130.24 (d), 130.99 (d), 131.31 (d), 132.75 (s), 137.45 (d), 152.62 (s), 157.45 (s). ^{29}Si NMR (53 MHz, $CDCl_3$) δ −58.08 (s). Anal. Calcd for $C_{18}H_{24}N_2O_3Si$: C, 62.76; H, 7.02; N, 8.13. Found: C, 62.65; H, 6.98; N, 8.18%.

Dimethyl[2-((*E*)-phenylazo)phenyl]silane ((*E*)-2e): Red oil. ^{1}H NMR (500 MHz, $CDCl_3$) δ 0.44 (d, $^3J_{HH}$ = 3.8 Hz, 6H), 4.69 (sept, $^3J_{HH}$ = 3.8 Hz, 1H), 7.45 (dt, $^3J_{HH}$ = 7.5 Hz, $^4J_{HH}$ = 1.5 Hz, 1H), 7.48−7.55 (m, 4H), 7.76 (dd, $^3J_{HH}$ = 7.5 Hz, $^4J_{HH}$ = 1.5 Hz, 1H), 7.83 (d, $^3J_{HH}$ = 7.5 Hz, 1H), 7.94 (d, $^3J_{HH}$ = 7.5 Hz, 2H). ^{13}C NMR (125 MHz, $CDCl_3$) δ −2.24 (q), 116.74 (d), 123.07 (d), 129.15 (d), 130.30 (d), 130.35 (d), 130.99 (d), 135.83 (d), 138.51 (s), 152.48 (s), 157.18 (s). ^{29}Si{^{1}H} NMR (53 MHz, $CDCl_3$) δ −16.95 (s). Anal. Calcd for $C_{14}H_{16}N_2Si$: C, 69.95; H, 6.71; N, 11.65. Found: C, 69.73; H, 6.76; N, 11.39%.

Diphenyl[2-((*E*)-phenylazo)phenyl]silane ((*E*)-2f): Red crystals (hexane), mp 74−75 °C. ^{1}H NMR (500 MHz, $CDCl_3$) δ 5.71(s, $^1J_{SiH}$ = 207.5 Hz, 1H), 7.28−7.37 (m, 9H), 7.42−7.46 (m, 3H), 7.54 (dd, $^3J_{HH}$ = 7.5 Hz, $^4J_{HH}$ = 1.5 Hz, 4H), 7.57−7.60 (m, 2H), 7.94 (dd, $^3J_{HH}$ = 7.5 Hz, $^4J_{HH}$ = 1.5 Hz, 1H). ^{13}C NMR (126 MHz, $CDCl_3$) δ 118.91 (d), 122.95 (d), 127.83 (d), 128.79 (d), 129.29 (d), 130.56 (d), 130.85 (d), 131.11 (d), 133.11 (s), 134.82 (s), 135.67 (d), 138.03 (d), 152.04 (s), 157.02 (s). ^{29}Si{^{1}H} NMR (53 MHz, $CDCl_3$) δ −19.90 (s). Anal. Calcd for $C_{24}H_{20}N_2Si$: C, 79.08; H, 5.53; N, 7.69. Found: C, 79.06; H, 5.60; N, 7.89%.

Diethoxyphenyl[2-((*E*)-phenylazo)phenyl]silane ((*E*)-2g): Red crystals (hexane), mp 55−56 °C. ^{1}H NMR (500 MHz, $CDCl_3$) δ 1.18 (t, $^3J_{HH}$ = 7.5 Hz, 6H), 3.82 (q, $^3J_{HH}$ = 7.5 Hz, 4H), 7.25−7.32 (m, 3H), 7.37−7.39 (m, 3H), 7.51 (t, $^3J_{HH}$ = 7.5 Hz, 1H), 7.55 (t, $^3J_{HH}$ = 7.5 Hz, 1H), 7.60−7.61 (m, 2H), 7.64 (dd, $^3J_{HH}$ = 7.5 Hz, $^4J_{HH}$ = 1.5 Hz, 2H), 7.77 (d, $^3J_{HH}$ = 7.5 Hz, 1H), 8.10 (d, $^3J_{HH}$ = 7.5 Hz, 1H). ^{13}C NMR (126 MHz, $CDCl_3$) δ 18.30 (q), 58.94 (t), 115.32 (d), 127.59 (d), 128.84 (d), 129.65 (d), 130.37 (d), 130.86 (d), 131.35 (d), 134.44 (s), 134.49 (d), 134.88 (s), 137.26 (d), 152.45 (s), 157.38 (s). ^{29}Si NMR (99 MHz, $CDCl_3$) δ −32.64 (s). Anal. Calcd for $C_{22}H_{24}N_2O_2Si$: C, 70.18; H, 6.42; N, 7.44. Found: C, 70.12; H, 6.40; N, 7.27%.

Dimethylbis[2-((*E*)-phenylazo)phenyl]silane ((*E*,*E*)-3a): Red crystals (hexane), mp 122−123 °C. ^{1}H NMR (500 MHz, $CDCl_3$)

(32) Badger, G. M.; Drewer, R. J.; Lewis, G. E. *Aust. J. Chem.* **1964**, *17*, 1036.

δ 0.69 (s, 6H), 7.35−7.39 (m, 8H), 7.43 (dt, $^3J_{HH}$ = 7.5 Hz, $^4J_{HH}$ = 1.5 Hz, 2H), 7.53−7.55 (m, 4H), 7.69 (dd, $^3J_{HH}$ = 7.5 Hz, $^4J_{HH}$ = 1.5 Hz, 2H), 7.72 (dd, $^3J_{HH}$ = 7.5 Hz, $^4J_{HH}$ = 1.5 Hz, 2H). ^{13}C NMR (68 MHz, $CDCl_3$) δ 0.91 (q), 114.93 (d), 123.10 (d), 128.83 (d), 129.86 (d), 130.02 (d), 130.65 (d), 135.60 (d), 141.18 (s), 152.41 (s), 156.74 (s). ^{29}Si NMR (53 MHz, $CDCl_3$) δ −7.79 (s). Anal. Calcd for $C_{26}H_{24}N_4Si$: C, 74.25; H, 5.75; N, 13.32. Found: C, 74.16; H, 5.79; N, 13.41%.

Diphenylbis[2-((*E*)-phenylazo)phenyl]silane ((*E*,*E*)-3b): Red needles (hexane), mp 174.5−176 °C. ^{1}H NMR (500 MHz, $CDCl_3$) δ 7.08−7.16 (m, 8H), 7.20−7.29 (m, 8H), 7.32 (t, $^3J_{HH}$ = 7.5 Hz, 2H), 7.44 (dt, $^3J_{HH}$ = 7.5 Hz, $^4J_{HH}$ = 0.9 Hz, 2H), 7.56 (t, $^3J_{HH}$ = 7.5 Hz, 6H), 7.76 (d, $^3J_{HH}$ = 7.5 Hz, 2H). ^{13}C NMR (68 MHz, $CDCl_3$) δ 115.24 (d), 123.14 (d), 127.48 (d), 128.44 (d), 128.80 (d), 130.23 (d), 130.34 (d), 130.51 (d), 136.11 (s), 136.49 (d), 137.59 (d), 137.78 (s), 152.08 (s), 156.54 (s). ^{29}Si NMR (53 MHz, $CDCl_3$) δ −13.76 (s). Anal. Calcd for $C_{36}H_{28}N_4Si$: C, 79.38; H, 5.18; N, 10.29. Found: C, 79.09; H, 5.42; N, 10.19%.

Phenylbis[2-((*E*)-phenylazo)phenyl]silane ((*E*,*E*)-3c): Red oil. ^{1}H NMR (500 MHz, $CDCl_3$) δ 6.06 (s, $^1J_{SiH}$ = 219.0 Hz, 1H), 7.30−7.37 (m, 9H), 7.39 (t, $^3J_{HH}$ = 7.5 Hz, 2H), 7.49−7.55 (m, 6H), 7.59 (dd, $^3J_{HH}$ = 7.5 Hz, $^4J_{HH}$ = 1.5 Hz, 2H), 7.63 (dd, $^3J_{HH}$ = 7.5 Hz, $^4J_{HH}$ = 1.5 Hz, 2H), 7.93 (d, $^3J_{HH}$ = 8.0 Hz, 2H). ^{13}C NMR (126 MHz, $CDCl_3$) δ 118.42 (d), 122.94 (d), 127.74 (d), 128.74 (d), 128.95 (d), 130.38 (d), 130.51 (d), 130.73 (d), 135.07 (s), 135.68 (d), 136.07 (s), 137.57 (d), 152.10 (s), 156.68 (s). ^{29}Si{^{1}H} NMR (99 MHz, $CDCl_3$) δ −23.22 (s). HRMS (FAB) *m*/*z* calcd for $C_{30}H_{24}N_4Si$ $[M]^+$, 468.1770; found, 468.1741.

Synthesis of Trifluoro[2-((*E*)-phenylazo)phenyl]silane ((*E*)-4d). To an ethereal solution of triethoxy[2-((*E*)-phenylazo)-phenyl]silane **2d** (3.35 g, 9.72 mmol) was added BF_3·Et_2O (1.34 mL, 10.7 mmol), and the reaction mixture was stirred for 7 h. After the solvent was removed, distillation from the reaction mixture (0.1 mmHg, 200 °C) and subsequent recrystallization from hexane gave yellow crystals of (*E*)-**4d** (1.28 g, 49%). (*E*)-**4d**: Yellow crystals (hexane), mp 51−52 °C. ^{1}H NMR (500 MHz, $CDCl_3$) δ 7.54−7.60 (m, 3H), 7.68 (t, $^3J_{HH}$ = 7.5 Hz, 1H), 7.80 (dt, $^3J_{HH}$ = 7.5 Hz, $^4J_{HH}$ = 1.5 Hz, 1H), 8.01 (dd, $^3J_{HH}$ = 7.5 Hz, $^4J_{HH}$ = 1.5 Hz, 1H), 8.15 (dd, $^3J_{HH}$ = 7.5 Hz, $^4J_{HH}$ = 1.5 Hz, 2H), 8.18 (d, $^3J_{HH}$ = 7.5 Hz, 1H). ^{13}C{^{1}H} NMR (126 MHz, $CDCl_3$) δ 112.92 (q, $^2J_{CF}$ = 19.7 Hz, *C*Si), 123.60 (s, *C*H), 129.51 (s, *C*H), 130.50 (s, *C*H), 132.90 (s, *C*H), 133.26 (s, *C*H), 134.33 (s, *C*H), 138.47 (s, *C*H), 147.43 (s, *C*N), 156.01 (q, $^3J_{CF}$ = 5.2 Hz, *C*N). ^{19}F NMR (254 MHz, CD_2Cl_2) (rt) δ −140.53 (s, $^1J_{SiF}$ = 234.7 Hz, 3F); (−90 °C) δ −141.11 (d, $^2J_{FF}$ = 52.0 Hz, 2F), −137.13 (t, $^2J_{FF}$ = 52.0 Hz, 1F). ^{29}Si NMR (53 MHz, CD_2Cl_2) (rt) δ −91.21 (q, $^1J_{SiF}$ = 231.0 Hz); (−90 °C) δ −94.55 (q, $^1J_{SiF}$ = 231.0 Hz). Anal. Calcd for $C_{12}H_9F_3N_2Si$: C, 54.12; H, 3.41; N, 10.52. Found: C, 54.10; H, 3.56; N, 10.62%.

Synthesis of Difluorophenyl[2-((*E*)-phenylazo)phenyl]silane ((*E*)-4g). Similarly to the synthesis of (*E*)-**4d**, (*E*)-**4g** was synthesized from (*E*)-**2g** (312 mg, 0.827 mmol) and BF_3·Et_2O (0.20 mL, 1.6 mmol) in 67% yield. (*E*)-**4g**: Yellow crystals (hexane), mp 82−83 °C. ^{1}H NMR (500 MHz, $CDCl_3$) δ 7.22 (t, $^3J_{HH}$ = 8.0 Hz, 3H), 7.30−7.41 (m, 4H), 7.44 (dd, $^3J_{HH}$ = 7.5 Hz, $^4J_{HH}$ = 1.5 Hz, 2H), 7.65−7.71 (m, 3H), 7.80 (d, $^3J_{HH}$ = 8.0 Hz, 1H), 8.09 (d, $^3J_{HH}$ = 7.5 Hz, 1H), 8.22 (d, $^3J_{HH}$ = 8.0 Hz, 1H). ^{13}C{^{1}H} NMR (126 MHz, $CDCl_3$) δ 118.85 (t, $^2J_{CF}$ = 17.4 Hz, *C*Si), 123.05 (s, *C*H), 127.97 (s, *C*H), 128.96 (s, *C*H), 129.71 (s, *C*H), 130.45 (s, *C*H), 131.79 (s, *C*H), 132.47 (s, *C*H), 132.56 (t, $^2J_{CF}$ = 20.4 Hz, *C*Si), 132.94 (s, *C*H), 133.28 (s, *C*H), 137.81 (t, $^3J_{CF}$ = 2.4 Hz, *C*H), 148.72 (s, *C*N), 156.85 (t, $^3J_{CF}$ = 3.6 Hz, *C*N). ^{19}F NMR (376 MHz, $CDCl_3$) δ −142.85 (s, $^1J_{SiF}$ = 264.5 Hz); (−100 °C) δ −149.45 (br s, 1F), −131.29 (br s, 1F). ^{29}Si{^{1}H} NMR (99 MHz, $CDCl_3$) δ −47.75 (t, $^1J_{SiF}$ = 264.5 Hz). Anal. Calcd for $C_{18}H_{14}F_2N_2Si$: C, 66.64; H, 4.35; N, 8.64. Found: C, 66.67; H, 4.59; N, 8.47%.

Fluorophenylbis[2-((*E*)-phenylazo)phenyl]silane ((*E*,*E*)-3d). To a THF solution (5 mL) of (*E*,*E*)-**3c** (174 mg, 0.37 mmol) was added AgF (150 mg, 1.18 mmol) at rt, and the reaction mixture was stirred for 2 d. After filtration of insoluble materials through Celite and evaporation of the solvent, recrystallization of the residue from hexane gave orange crystals of (*E*,*E*)-**3d** (158 mg, 87%). (*E*,*E*)-**3d**: Orange crystals (hexane), mp 107−109 °C. ^{1}H NMR (500 MHz, $CDCl_3$) δ 7.20−7.27 (m, 7H), 7.31 (t, $^3J_{HH}$ = 7.5 Hz, 2H), 7.32−7.38 (m, 4H), 7.48 (td, $^3J_{HH}$ = 7.5 Hz, $^4J_{HH}$ = 1.5 Hz, 2H), 7.57 (dd, $^3J_{HH}$ = 7.5 Hz, $^4J_{HH}$ = 1.5 Hz, 2H), 7.71 (dd, $^3J_{HH}$ = 7.5 Hz, $^4J_{HH}$ = 1.5 Hz, 2H), 7.89 (d, $^3J_{HH}$ = 7.5 Hz, 2H), 7.94 (dd, $^3J_{HH}$ = 7.5 Hz, $^4J_{HH}$ = 1.5 Hz, 2H). ^{13}C{^{1}H} NMR (126 MHz, $CDCl_3$) δ 120.44 (s, *C*H), 122.80 (s, *C*H), 127.56 (s, *C*H), 128.49 (s, *C*H), 129.59 (s, *C*H), 130.60 (s, *C*H), 130.70 (s, *C*H), 130.76 (s, *C*H), 133.36 (d, $^2J_{CF}$ = 18.9 Hz, *C*Si), 134.98 (d, $^2J_{CF}$ = 20.0 Hz, *C*Si), 135.00 (d, $^4J_{CF}$ = 1.4 Hz, *C*H), 136.04 (d, $^3J_{CF}$ = 3.3 Hz, *C*H), 151.27 (s, *C*N), 156.27 (s, *C*N). ^{19}F NMR (254 MHz, $CDCl_3$) δ −151.13 (s, $^1J_{SiF}$ = 273.2 Hz). ^{29}Si{^{1}H} NMR (99 MHz, $CDCl_3$) δ −17.27 (d, $^1J_{SiF}$ = 273.2 Hz). Anal. Calcd for $C_{30}H_{23}N_4SiF$: C, 74.05; H, 4.76; N, 11.51. Found: C, 73.88; H, 5.00; N, 11.27%.

The fluorosilanes (*E*)-**4e** and (*E*)-**4f** were synthesized similarly from the hydrosilanes (*E*)-**2e** and (*E*)-**2f**, respectively.

Fluorodimethyl[2-((*E*)-phenylazo)phenyl]silane ((*E*)-4e): Brown oil. ^{1}H NMR (500 MHz, $CDCl_3$) δ 0.50 (d, $^3J_{FH}$ = 7.9 Hz, 6H), 7.51−7.57 (m, 4H), 7.63 (dt, $^3J_{HH}$ = 7.5 Hz, $^4J_{HH}$ = 1.5 Hz, 1H), 7.92−7.96 (m, 3H), 8.05 (d, $^3J_{HH}$ = 7.5 Hz, 1H). ^{13}C{^{1}H} NMR (126 MHz, $CDCl_3$) δ 1.27 (d, $^2J_{CF}$ = 19.6 Hz, *C*H$_3$), 122.83 (s, *C*H), 124.94 (s, *C*H), 129.32 (s, *C*H), 131.03 (s, *C*H), 131.24 (s, *C*H), 131.38 (s, *C*H), 131.92 (d, $^2J_{CF}$ = 16.6 Hz, *C*Si), 135.27 (d, $^3J_{CF}$ = 6.3 Hz, *C*H), 150.79 (s, *C*N), 156.29 (d, $^3J_{CF}$ = 2.1 Hz, *C*N). ^{19}F NMR (254 MHz, $CDCl_3$) δ −152.61 (sept, $^1J_{SiF}$ = 267.7 Hz, $^3J_{HF}$ = 7.9 Hz). ^{29}Si{^{1}H} NMR (53 MHz, $CDCl_3$) δ 8.27 (d, $^1J_{SiF}$ = 267.7 Hz). Anal. Calcd for $C_{14}H_{15}N_2SiF$: C, 65.08; H, 5.85; N, 10.84. Found: C, 65.26; H, 6.02; N, 10.68%.

Fluorodiphenyl[2-((*E*)-phenylazo)phenyl]silane ((*E*)-4f): Yellow crystals (hexane), mp 102−103 °C. ^{1}H NMR (500 MHz, $CDCl_3$) δ 7.15−7.19 (m, 4H), 7.23−7.28 (m, 5H), 7.32 (tt, $^3J_{HH}$ = 7.5 Hz, $^4J_{HH}$ = 1.2 Hz, 2H), 7.58 (dd, $^3J_{HH}$ = 7.5 Hz, $^4J_{HH}$ = 1.5 Hz, 4H), 7.63 (dt, $^3J_{HH}$ = 7.5 Hz, $^4J_{HH}$ = 1.5 Hz, 1H), 7.72 (dt, $^3J_{HH}$ = 7.5 Hz, $^4J_{HH}$ = 1.5 Hz, 1H), 8.12−8.14 (m, 2H). ^{13}C{^{1}H} NMR (126 MHz, $CDCl_3$) δ 122.77 (s, *C*H), 125.22 (s, *C*H), 127.83 (s, *C*H), 128.63 (s, *C*H), 129.90 (s, *C*H), 130.89 (s, *C*H), 131.65 (s, *C*H), 131.98 (s, *C*H), 134.42 (d, $^2J_{CF}$ = 1.6 Hz, *C*Si), 134.56 (s, *C*H), 134.73 (s, *C*H), 137.12 (d, $^2J_{CF}$ = 5.6 Hz, *C*Si), 150.63 (s, *C*N), 157.04 (s, *C*N). ^{19}F NMR (254 MHz, $CDCl_3$) δ −152.14 (s, $^1J_{SiF}$ = 273.6 Hz). ^{29}Si NMR (99 MHz, $CDCl_3$) δ −16.25 (d, $^1J_{SiF}$ = 273.6 Hz). Anal. Calcd

for $C_{24}H_{19}FN_2Si$: C, 75.36; H, 5.01; N, 7.32. Found: C, 75.60; H, 5.16; N, 7.35%.

Synthesis of Potassium, 18-Crown-6 Tetrafluoro[2-((*E*)-phenylazo)phenyl]silicate ((*E*)-5). To a toluene solution (2.5 mL) of (*E*)-**4d** (100 mg, 0.376 mmol) were added KF (21.8 mg, 0.376 mmol) and 18-crown-6 (99.3 mg, 0.376 mmol) at room temperature, and the reaction mixture was stirred for 26 h. Recrystallization of the resulting yellow precipitates from $CHCl_3$/ether gave yellow crystals of silicate (*E*)-**5** (164 mg, 74%). (*E*)-**5**: Yellow crystals ($CHCl_3/Et_2O$), mp 185−186 °C. ^{1}H NMR (500 MHz, $CDCl_3$) δ 3.55 (s, 24H), 7.30 (t, $^3J_{HH}$ = 7.2 Hz, 1H), 7.36−7.38 (m, 3H), 7.45 (t, $^3J_{HH}$ = 7.2 Hz, 1H), 7.71 (d, $^3J_{HH}$ = 6.7 Hz, 1H), 7.96 (d, $^3J_{HH}$ = 7.3 Hz, 1H), 8.11−8.13 (m, 2H). ^{13}C{^{1}H} NMR (126 MHz, $CDCl_3$) δ 69.87 (s), 123.91 (s), 126.34 (s), 127.98 (s), 129.52 (s), 129.58 (s), 130.57 (s), 133.18 (s), 142.47 (quint, $^2J_{CF}$ = 40.3 Hz), 149.99 (s), 152.24 (s). ^{19}F NMR (254 MHz) (50 °C, $CDCl_3$) δ −127.40 (s, $^1J_{SiF}$ = 189.0 Hz); (−90 °C, CD_2Cl_2) δ −147.17 (dt, $^2J_{FF}$ = 21.3 Hz, $^2J_{FF}$ = 24.4 Hz, 1F), −123.18 (d, $^2J_{FF}$ = 24.4 Hz, 2F), −121.63 (d, $^2J_{FF}$ = 21.3 Hz, 1F). ^{29}Si{^{1}H} NMR (53 MHz) (rt, $CDCl_3$) δ −150.88 (quint, $^1J_{SiF}$ = 192.5 Hz); (−90 °C, CD_2Cl_2) δ −153.73 (ddt, $^1J_{SiF}$ = 148.9 Hz, $^1J_{SiF}$ = 185.7 Hz, $^1J_{SiF}$ = 213.9 Hz). Anal. Calcd for $C_{24}H_{33}F_4KN_2O_6Si$: C, 48.96; H, 5.65; N, 4.76. Found: C, 48.69; H, 5.49; N, 4.92%.

Photoisomerization of (*E*)-4d: A $CDCl_3$ solution (80 mM, 0.5 mL) of (*E*)-**4d** in a 5 mmϕ NMR tube was irradiated with high-pressure mercury lamp through a colored-glass filter (λ = 360 nm) for 1 h in the dark room. The color of the reaction solution gradually changed from yellow to red during the irradiation. In ^{19}F NMR spectra, a broad signal at δ −140.6 decreased, and a new sharp singlet was observed at δ −138.0, which was assigned as (*Z*)-**4d**.[12] Ratio of (*E*)-**4d**/(*Z*)-**4d** was determined to be 19:81 by integral of the ^{19}F NMR spectra. After the reaction solution was kept at rt for 6 h in the dark, (*Z*)-**4d** completely disappeared and (*E*)-**4d** was recovered quantitatively. Irradiation (λ = 431 nm) of the mixture of (*E*)-**4d** and (*Z*)-**4d** for 3 h changed the ratio of (*E*)-**4d**/(*Z*)-**4d** to 100:0. Photoisomerizations of (*E*)-**4e**−**g** (10 mM, 0.5 mL) and (*E*)-**5** (40 mM, 0.5 mL) to the corresponding (*Z*)-isomers were carried out similarly.

(*Z*)-4e: Red solution (in $CDCl_3$). ^{1}H NMR (500 MHz, $CDCl_3$) δ 0.60 (d, $^3J_{FH}$ = 7.7 Hz, 6H), 6.11 (d, $^3J_{HH}$ = 8.0 Hz, 1H), 6.85 (d, $^3J_{HH}$ = 7.5 Hz, 2H), 7.06 (t, $^3J_{HH}$ = 7.5 Hz, 1H), 7.16−7.25 (m, 4H), 7.75 (d, $^3J_{HH}$ = 7.5 Hz, 1H). ^{13}C{^{1}H} NMR (126 MHz, $CDCl_3$) δ −0.18 (d, $^2J_{CF}$ = 14.3 Hz, *C*H$_3$), 115.75 (s, *C*H), 120.32 (s, *C*H), 127.19 (s, *C*H), 127.53 (s, *C*H), 128.79 (s, *C*H), 129.87 (s, *C*H), 134.52 (s, *C*H), 135.24 (d, $^2J_{CF}$ = 10.5 Hz, *C*Si), 153.28 (s, *C*N), 158.03 (s, *C*N). ^{19}F NMR (376 MHz, $CDCl_3$) δ −163.12 (sept, $^1J_{SiF}$ = 273.7 Hz, $^3J_{FH}$ = 7.7 Hz); ^{29}Si{^{1}H} NMR (99 MHz, $CDCl_3$) δ 21.01 (d, $^1J_{SiF}$ = 273.7 Hz).

(*Z*)-4f: Red crystals (hexane). ^{1}H NMR (500 MHz, $CDCl_3$) δ 6.11 (d, $^3J_{HH}$ = 7.5 Hz, 1H), 6.53 (d, $^3J_{HH}$ = 7.5 Hz, 2H), 7.09 (t, $^3J_{HH}$ = 7.5 Hz, 2H), 7.16 (t, $^3J_{HH}$ = 7.5 Hz, 2H), 7.22 (t, $^3J_{HH}$ = 7.5 Hz, 1H), 7.38−7.45 (m, 6H), 7.81 (dd, $^3J_{HH}$ = 7.5 Hz, $^4J_{HH}$ = 1.5 Hz, 4H), 7.94 (d, $^3J_{HH}$ = 7.5 Hz, 1H). ^{19}F NMR (254 MHz, $CDCl_3$) δ −170.58 (s, $^1J_{SiF}$ = 275.7 Hz). ^{29}Si-{^{1}H} NMR (99 MHz, $CDCl_3$) δ −7.29 (d, $^1J_{SiF}$ = 275.7 Hz).

(*Z*)-4g: ^{1}H NMR (500 MHz, $CDCl_3$) δ 6.16 (d, $^3J_{HH}$ = 7.5 Hz, 1H), 6.79 (d, $^3J_{HH}$ = 7.5 Hz, 2H), 7.16−7.19 (m, 2H), 7.21−7.26 (m, 3H), 7.44 (t, $^3J_{HH}$ = 7.5 Hz, 2H), 7.51 (t, $^3J_{HH}$ = 7.5 Hz, 1H), 7.88 (dd, $^3J_{HH}$ = 7.5 Hz, $^4J_{HH}$ = 1.5 Hz, 2H), 7.94 (dd, $^3J_{HH}$ = 7.5 Hz, $^4J_{HH}$ = 1.5 Hz, 1H). ^{19}F NMR (254 MHz, $CDCl_3$) δ −140.36 (s, $^1J_{SiF}$ = 287.5 Hz). ^{29}Si{^{1}H} NMR (99 MHz, $CDCl_3$) δ −29.80 (t, $^1J_{SiF}$ = 287.5 Hz).

(*Z*)-5: Red crystals (THF/Et_2O). ^{1}H NMR (500 MHz, $CDCl_3$) δ 3.57 (s, 24H), 5.89 (d, $^3J_{HH}$ = 7.6 Hz, 1H), 6.84 (t, $^3J_{HH}$ = 7.6 Hz, 1H), 6.97−7.04 (m, 4H), 7.15 (t, $^3J_{HH}$ = 7.8 Hz, 2H), 7.80 (d, $^3J_{HH}$ = 6.7 Hz, 1H). ^{13}C{^{1}H} NMR (126 MHz, $CDCl_3$, −65 °C) δ 69.52 (s), 115.38 (s), 120.85 (s), 125.35 (s), 126.43 (s), 127.33 (s), 127.99 (s), 134.35 (s), 135.79 (quint, $^2J_{CF}$ = 35.9 Hz), 153.09 (s), 158.04 (s). ^{19}F NMR (254 MHz, $CDCl_3$) δ −114.71 (s).

Photoisomerization of (*E*,*E*)-3d: Similarly, a $CDCl_3$ solution (5 mM, 0.5 mL) of (*E*,*E*)-**3d** was irradiated (λ = 360 nm) for 12 h to give fluorophenyl[2-((*E*)-phenylazo)phenyl][2-((*Z*)-phenylazo)phenyl]silane ((*E*,*Z*)-**3d**) and fluorophenylbis[2-((*Z*)-phenylazo)phenyl]silane ((*Z*,*Z*)-**3d**) ((*E*,*E*)-**3d**/(*E*,*Z*)-**3d**/(*Z*,*Z*)-**3d** = 13:15:72). (*E*,*Z*)-**3d**: ^{19}F NMR (254 MHz, $CDCl_3$) δ −151.59 (brs, $^1J_{SiF}$ = 275.7 Hz). (*Z*,*Z*)-**3d**: ^{19}F NMR (254 MHz, $CDCl_3$) δ −166.76 (s, $^1J_{SiF}$ = 275.7 Hz).

Reactions of (*E*)- and (*Z*)-5 with BF_3·OEt_2: To a $CDCl_3$ solution (0.5 mL) of (*E*)-**5** (5.9 mg, 0.010 mmol) was added BF_3·Et_2O (10 μL, 0.079 mmol). Quantitative formation of (*E*)-**4d** and a tetrafluoroborate ion was observed in the ^{1}H and ^{19}F NMR spectra after 5 min. The reaction of (*E*)-**5** gave the same results.

X-ray Crystallographic Analyses of (*E*)-2c, (*E*)-2f, (*E*,*E*)-3a, (*E*)-4d, (*E*)-4f, (*E*)-4 g, (*Z*)-4f, (*E*)-5, and (*Z*)-5: All data for (*E*)-**2c**, (*E*)-**2f**, (*E*,*E*)-**3a**, (*E*)-**4d**, (*E*)-**4f**, (*E*)-**4g**, (*Z*)-**4f**, (*E*)-**5**, and (*Z*)-**5** were recorded on a Rigaku Mercury CCD diffractometer with graphite monochromated Mo Kα radiation (λ = 0.710 70 Å). Data were collected and processed using CrystalClear (Rigaku). The data were corrected for Lorentz and polarization effects. The structure was solved by direct methods (SHELX-97) and expanded using Fourier techniques.[33] The non-hydrogen atoms were refined anisotoropically. Hydrogen atoms were refined isotropically. Crystallographic data are summarized in Table 2.

Acknowledgment. We thank Shin-etsu Chemical Co., Ltd., and Tosoh Finechem Corporation for the gifts of chlorosilanes and alkyllithiums, respectively. This work was partially supported by Grant-in-Aid for The 21st Century COE Program for Frontiers in Fundamental Chemistry (T.K.) and for Scientific Research Nos. 15036217 (T.K. and N.K.) and 16033216 (T.K. and N.K.) from Ministry of Education, Culture, Sports, Science and Technology, Japan. This work was also supported by Dainippon Ink & Chemicals, Incorporated and by Grant-in-Aid for Scientific Research Nos. 15105001 (T.K.), 14740395 (N.K.), and 1611512 (M.Y.) by the Japan Society for the Promotion of Science.

Supporting Information Available: Details of crystallographic analyses of compounds (*E*)-**2c**, (*E*)-**2f**, (*E*,*E*)-**3a**, (*E*)-**4d**, (*E*)-**4f**, (*E*)-**4g**, (*Z*)-**4f**, (*E*)-**5** and (*Z*)-**5** in CIF format. This material is available free of charge via the Internet at http://pubs.acs.org.

JA060926S

(33) Sheldrick, G. M. *SHELXL-97, Program for the Refinement of Crystal Structures*; University of Göttingen: Göttingen, Germany, 1997.